9

Properties and Applications of Ceramic Composites Containing Silicon Carbide Whiskers

Brian D. Bertram and Rosario A. Gerhardt
Georgia Institute of Technology
United States of America

1. Introduction

In the early 1980s, researchers at Oak Ridge National Laboratory developed a new type of ceramic composite reinforced with dispersed silicon carbide (SiC) whiskers. The majority-phase ("matrix") material of these composites was aluminum oxide (Al_2O_3) and the minority-phase ("filler") SiC was grown in whisker-form by a pyrolysis technique using organic waste such as rice hulls. Inclusion of a small volume fraction of silicon carbide whiskers (SiC_w) in Al_2O_3 had a large impact on the properties and allowed for interesting applications which otherwise would not be possible with Al_2O_3 alone. The whisker form of SiC made the composites exceptionally non-brittle compared to conventional monolithic ceramics due to a variety of toughening mechanisms within the composites. Many years later, it was discovered that the whiskers also imparted useful electrical properties.

The invention of the composites roughly coincided with the U.S. Department of Energy's development of the 1983 "Ceramic Technology Program for Advanced Heat Engines" (Sinott, 1987). A few years earlier, President Carter pushed for the development of more fuel-efficient automobiles to mitigate the energy problems of the United States(Carter, 1977) which were earlier noted by President Ford(Ford, 1975). Ceramic engines operating at high temperatures have the potential for high energy efficiency due to the thermodynamics of engine operation(DeHoff, 1993) and the whisker-reinforced composites were candidate materials for this purpose. However, subsequent research found that significant degradation of the whisker-laden composites occurred during extended exposure to stress and air at high temperatures due to reaction of the SiC whiskers, leading to extensive deformation by creep phenomena. Such structural degradation was correlated to worsening of mechanical properties and the development of Al_2O_3-SiC_w composites for engines stalled. However, Al_2O_3-SiC_w composites have been found to be useful and commercially viable as cutting tools and microwave-heating inserts. In working towards these applications, a large amount of research has been conducted on this composite system: the literature contains many different perspectives on the material. In considering the implications of the different perspectives, one can develop new insights. The goal of this chapter is to distill the most

significant results of the literature and create a big-picture description of these materials for readers having some background in materials science.

2. SiC Whiskers

2.1. SiC Whisker Fabrication

The term 'whisker' is commonly used to describe a small single-crystalline rod. SiC whiskers may be synthesized by various methods, such as sol-gel, plasma deposition, chemical vapor deposition, and pyrolysis of agricultural waste. The latter method seems to be preferred for industrial-scale production of SiC whiskers. Generally, agricultural waste containing both silica (SiO_2) and carbon is used. Waste sources include rice hulls, coconut shells, bean-curd refuse, sugarcane leaf, and rice straw. Silicon carbide whiskers can also be fabricated from mixtures of silica and carbon powders, carbon and silicon halides, polymer precursors, or other materials like silicon nitride. In addition to SiC whiskers, the synthesis process also usually produces some amount of (usually unwanted) non-whisker SiC particles which varies depending on processing details. After synthesis, whiskers are often cleaned by ultrasonication (Raju & Verma, 1997) and/or acid washing (Raju & Verma, 1997; Ye et al., 2000) to remove contamination of particulates (Lee & Sheargold, 1986) and trace amounts of amorphous silica which often remain on the whiskers (Raju & Verma, 1997).

Synthesis from rice hulls may be conducted in the 1000-1500°C range in an inert gas ambient, e.g. N_2 (Raju & Verma, 1997). In another work, a 700-800°C carbonization pretreatment of the organic waste was performed to increase carbon surface area before conducting the 1400°C pyrolysis in argon (Singh et al., 1998). Reaction occurs when silica (SiO_2) undergoes a carbothermic reduction to SiC. The overall reaction is given by Reaction 1 and the related sub-reactions (2-4) are:

(1): $SiO_2 + 3C \rightarrow SiC + 2CO_{(g)}$

(2): $SiO_{(g)} + 2C \rightarrow SiC + CO_{(g)}$

(3): $SiO_{(g)} + C \rightarrow Si + CO_{(g)}$

(4): $Si + C \rightarrow SiC$

It is believed that silica is first reduced to gaseous SiO (i.e. $SiO_2 + C \rightarrow SiO_{(g)} + CO_{(g)}$), and then forms SiC either by a replacement reaction (#2) or through the continued reduction to Si (Reaction #3) and subsequent addition reaction (#4) (Raju & Verma, 1997). The initial reaction between carbon and the silica (or silica derivative) depends upon the physical contact between the two. Ideally, the silica should be intimately mixed with the cellulose. As the reduction reaction proceeds, the intimate contact between silica and carbon is lost and further reduction of silica depends mainly on the gas-phase carbon source. Certain waste, such as coconut shells, are believed to produce more carbonaceous vapours (e.g. CO) for more efficient carbothermal reduction and higher yield. It is believed that the porous cellular structure of rice hulls facilitates vapor-phase transport. To achieve high-yield, it seems important to achieve a certain balance of silica:carbon in the starting materials (Raju & Verma, 1997; Singh et al., 1998).

A small amount of metal catalyst may be mixed in with the source materials for SiC whisker synthesis. This can be done by soaking the raw ingredients in an appropriate metal-salt

solution. Examples of metals include iron, Pd, Ni, or Co. Catalysts generally promote whisker growth by the vapor-liquid-solid (VLS) mechanism, which is fairly well-established in the growth of "1-dimensional" materials such as nanowires and nanotubes (Wagner & Ellis, 1964). For SiC whiskers, the theory implies that Si- and C-containing vapors dissolve into the molten metal catalyst balls and SiC precipitates when the solution becomes sufficiently supersaturated. This is then followed by unidirectional growth in the energetically-favored crystallographic direction. However, it should be noted that it is possible to grow SiC whiskers without such catalysts and these are believed to grow by a vapor-solid mechanism (Singh et al., 1998). Such whiskers tend to exhibit pointed tips at the ends and are not capped with catalyst balls, unlike VLS-grown whiskers.

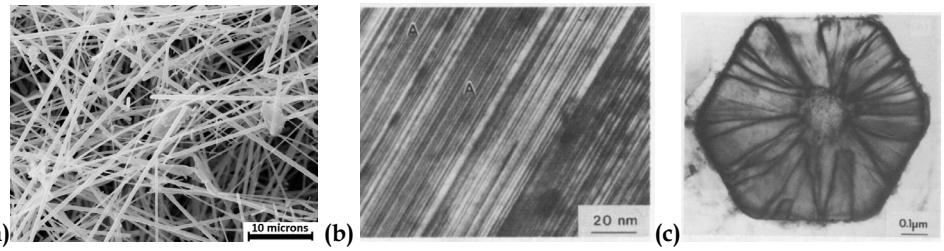

Fig. 1. Electron micrographs of (a) loose as-grown SiC whiskers, (b) planar defects perpendicular to the length of a single SiC whisker, and (c) a whisker cross-section showing partial dislocations and core cavities. *Sources*: (a) the Greenleaf Corporation and (b & c) S. R. Nutt, 1988; John Wiley & Sons, with permission.

2.2. SiC Whisker Structure

Figure 1a shows an image of as-grown SiC whiskers. Typically, SiC whiskers have lengths and diameters on the order 5-50 μm and 0.2-1.0 μm, respectively. The crystal structure of SiC may be described by a polytype. Broadly, the SiC polytypes may be categorized as β (cubic, i.e. zinc-blende) or α (non-cubic, e.g. hexagonal). However, there are many other SiC_w structural characteristics to consider. Generally, the whisker morphology and structure of the SiC particles results from the growth process (Nutt, 1984, 1988; Porter & Davis, 1995).

The structure and defects of silicon carbide whiskers made from rice hulls have been studied by transmission electron microscopy and this provided insight into their atomic- and nano-structure (Nutt, 1984). The whiskers were found to have grown in the <111> direction and exhibited a high density of planar defects such as stacking faults and twins on the {111} planes. As shown in Figure 1b, the spacings between planar faults in SiC_w may be as small as a few nm.The presence of these planar defects mean that the whisker structure may be described as a complex mixture of α and β polytypes arranged in thin lamellae perpendicular to the growth axes. However, it is common for whiskers to be reported as being of a single polytype (ACM website; Bertram & Gerhardt, 2010; Mebane & Gerhardt, 2004) based on x-ray diffraction phase identifications and reports from the manufacturer. Currently, the leading SiC_w manufacturer in the United States is Advanced Composite Materials LLC in Greer, SC.

Other common SiC_w defects include core cavities and partial dislocations,(Nutt, 1984) as shown in Figure 1c. The size range for core-cavities and voids was 2-20 nm. Whiskers were found to have hexagonal facetting, likely traceable to anisotropy in the surface energy during SiC crystal formation. Other studies indicate that as-fabricated whiskers may contain small pockets of silicon oxycarbide glass (Karunanithy, 1989). Generally speaking, whisker structure and arrangement can have significant effects on composite properties. Rice provides a more general review of ceramic (and metal) whisker growth and points out that for general growth of inorganic crystals, the morphology and growth habits are affected by impurities in the growth environment (Rice, 2003).

2.3. Health Risk of Loose SiC Whiskers

Finally, it should be noted that the loose whisker morphology (i.e. when the whiskers are not incorporated in solid composites) gives rise to a serious respiratory health risk and that unsafe handling of loose SiC whiskers can lead to deadly lung diseases (Rodelsperger & Bruckel, 2006; Vaughan & Trently, 1996). Generally, the elongated shapes (high aspect ratio), small sizes (micron level), and the facts that they are chemically inert and cannot be readily removed by natural human-body processes make SiC whiskers behave similarly to asbestos when in the lungs. Therefore it is of utmost importance to take care when working with loose whiskers or whisker-laden powders and to avoid stirring them up into the air. Also, one should always employ engineering controls (e.g. filtered respirators, specialized hoods) to minimize human inhalation and exposure during handling. However, certain whisker-containing composites used for cooking food have been NSF-51 approved for food contact. Currently, this technology is being marketed as Silar© by Advanced Composite Materials LLC.

3. Ceramic Composites Reinforced with Silicon Carbide Whiskers

The incorporation of SiC_w into ceramic composites generally results in an improvement in properties compared to the monolithic matrix. However, the behavior of SiC_w-filled ceramic composites depends on many factors and this requires one to consider them from numerous different perspectives in order to understand the behavior. To this end, we begin by considering their ultimate purposes / applications. Once, Al_2O_3-SiC_w composites had prospective application (Sinott, 1987) in high-temperature ceramic engines, and for this one would be interested in responses to creep, thermal shock, and fatigue. Currently, the commercial applications of Al_2O_3-SiC_w are in cutting tools and microwave-heating inserts.

3.1. Cutting-Tool Application

Images of Al_2O_3-SiC_w cutting-tool inserts are shown in Figure 2a. Cutting tools usually must be hot-pressed to achieve full density and the necessary thermal-mechanical properties. Such tools are cost-effective for shaping difficult-to-machine metals such as steel (Figure 2b) and Ni-based superalloys for turbines in aerospace applications. For the cutting tool application, one is generally interested in the following properties of the composite: fracture toughness, thermal conductivity, abrasive wear resistance, chemical inertness, and thermal shock resistance (which depends on fracture toughness and thermal conductivity). Compared to conventional ceramics, Al_2O_3-SiC_w composites provide improvements

(increases) in all the above properties except chemical inertness. During cutting with tools of Al_2O_3-SiC_w, damage is accompanied by whisker toughening mechanisms and reaction may occur between SiC and Fe. This generally limits cutting of ferrous materials to lower speeds (Collin & Rowcliffe, 2001; Thangaraj & Weinmann, 1992).

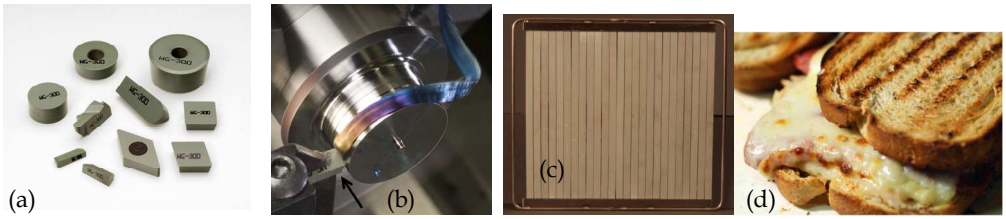

Fig. 2. Applications of Al_2O_3-SiC_w composites: (a) cutting-tool inserts, (b) insert (marked with arrow) machining hardened tool steel, (c) microwave flatstone, (d) panini sandwich speed-grilled with Silar© technology. Images provided by Greenleaf Corporation in Saegertown, PA (a,b) and Advanced Composite Materials LLC in Greer, SC (c,d).

Notably, the general cutting process is complicated and depends on many factors (Li, 1994; Mehrotra, 1998), including the defect distribution in the tool, tool shape, and the properties of the piece being cut. Also, there are different types of tool degradation which depend on the location on the tool. For SiC_w-reinforced tools, literature suggests that the residual stresses in the microstructure are rather important in determining mechanical and wear response, e.g. at the sample surface and at whisker-matrix interfaces(Billman et al., 1988; Thangaraj & Weinmann, 1992). It has also been found that wear performance depends on sample orientation relative to the processing direction and fracture toughness at the microstructural level, not the fracture toughness of the bulk sample (Dogan & Hawk, 2000). Moreover, one may use a lamination process to increase control of the Al_2O_3-SiC_w microstructure and thus improve cutting tool performance (Amateau et al., 1995). Also, tools employing specially-coated whiskers can provide increased toughness, tool life, and cutting speed. These may be obtained from the Greenleaf Corporation.

3.2. Application in Microwave Heating and Cooking

Currently, the microwave application is led by Advanced Composite Materials LLC in Greer, SC (Quantrille, 2007, 2008). For this application, density and mechanical properties are not as important and composite rods or bars ~1 foot long and ~½ inch wide are made by extrusion and pressureless sintering. Several rods are then arranged with a metal clip to form a grill or flatstone like that shown in Figure 2c which is then placed in a microwave oven having a clip-compatible design. Food products such as fresh dough pizza and panini sandwiches can then be cooked faster to yield a high quality result (e.g. crispy crust, grill marks, etc.) with application of microwave radiation (e.g. at 0.915, 2.45 GHz) in the cavity. An example is shown in Figure 2d. The microwaves preferentially heat the ceramic composite compared to the food. This is because, generally, the solid food on the grill has a much-reduced dielectric loss compared to the ceramic composite. The dielectric loss of the solid food can be expected to follow mainly from moisture and oil content (Basak & Priya, 2005; Metaxas & Meredith, 1983; Quantrille, 2008). For the composites, the dielectric loss primarily depends on the properties of the dispersed SiC_w population and is proportional to

the microwave heating rate of the composite. The literature suggests that composite thermal conductivity and thermal shock response may influence food heating during cooking and the lifetime of the parts, respectively (Basak & Priya, 2005; Parris & Kenkre, 1997) (McCluskey et al., 1990) (W. J. Lee & Case, 1989; Quantrille, 2007, 2008).

Quantrille has analyzed the heat transfer into the food during cooking and reported results of various microwave heating tests (Quantrille, 2007, 2008). The ceramics heat quickly, e.g. at ~2.3-4.6 °C/s from 900 W incident on powders blends of 7.5-15 wt% SiC_w in Al_2O_3. Food heating results from three processes: (1) dielectric loss in the food itself (2) air convection from the ceramic and (3) thermal conduction across the thermal gradient at the ceramic-food interface. Due to (3) and the fact that food moisture content declines as cooking proceeds, it is possible to sear the food with grill marks at the end of cooking. It was found that pizzas and paninis could be "grilled, toasted, and cooked to perfection" in ~80 and ~90 seconds, respectively (Quantrille, 2008). This method can also reduce the energy cost of cooking compared to conventional methods.

3.3. Introduction to Structure-Property Relations of Composites

To understand different types of models for SiC_w composites, it is useful to know the broader context of composite-material modeling (Jones, 1984; Mallick, 2008; Runyan et al, 2001a, 2001b; Taya, 2005). Most models depend in some way on the spatial distribution of the phases. Common distributions are shown in Figure 2.

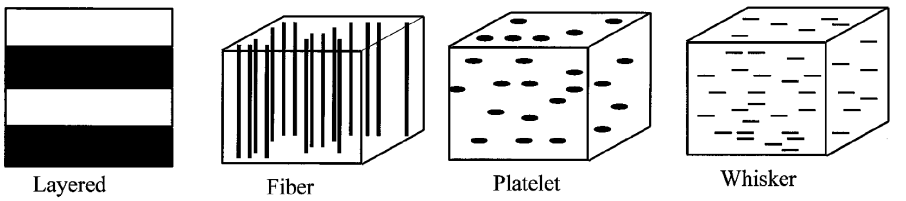

Fig. 3. Common types of composite structures. Here, "Fiber" implies continuous unidirectional fibers. After Runyan et al., 2001a, with permission (John Wiley & Sons).

Model complexity can vary a great deal based on the extent of assumptions made in the model development. The simplest models are the mixing rules which are applicable when the second phase has a unidirectional and continuous morphology, e.g. layered and fiber composites, as shown in Figure 3. These models result in the composite material response properties being predicted as volume-fraction (V) weighted averages of the properties of the constituent phases. Specifically, many properties may be modeled via

$$G_M = V_0G_0 + V_1G_1 \tag{5}$$

$$1/H_M = V_0/H_0 + V_1/H_1 \tag{6}$$

where G relates to the response along the fiber/phase alignment direction and H relates to the response in the transverse direction. Here, subscripts '0' and '1' denote phase 0 (the matrix) and phase 1 (the filler)and 'M' denotes the composite mixture. Equation 5 can be

applied to model how mechanical stress is distributed among the two phases of a fiber composite loaded in the fiber direction when the isostrain condition is applicable. Or, it may be used to model the electrical resistivity of two phases in series (e.g. layered composites). Equation 6 can be used to model the effective elastic modulus of fibrous composites in the direction perpendicular to the fibers. Or, it may be used to model the effective resistivity of two phases in parallel (e.g. layered composites). In principle, these mixing laws can predict many properties if the materials and structure are consistent with the assumptions of the mixing law. The interested reader should consult the following references, especially for mechanical properties (Jones, 1999; Mallick, 2008). Taya provides a nice treatment of electrical modeling and the physics, continuum mechanics, and mathematics principles which underlie modeling efforts in general (Taya, 2005).

For composites having a discontinuous dispersed second phase (e.g. platelet- or whisker-like filler, as shown in Figure 3) effective medium theory is more applicable. Compared to mixing rules, effective medium theories employ a different perspective: they use descriptions of the effects of inclusions on the relevant stress and/or strain fields in the bulk material to deduce related macroscopic materials properties. For example, they may relate the local electric and magnetic fields around conductive filler particles to the electromagnetic response of the composite, or alternatively, the mechanical stress-strain fields around reinforcement particles to the composite mechanical response. In other words, these theories attempt to generalize outward from descriptions of the small-scale situations to predict the effective macroscopic response of the composite mixtures. State-of-the-art theories (Lagarkov & Sarychev, 1996) have been found to provide fair to very-good agreement with experimental data from complicated dispersed-rod composite structures.(Lagarkov et al, 1997, 1998; Lagarkov & Sarychev, 1996) For fracture-toughness modeling, one reference stands out (Becher et al., 1989). Newcomers to electrical modeling may find that other references provide a better introduction to these topics (Gerhardt, 2005; Jonscher, 1983; Metaxas & Meredith, 1983; Runyan et al., 2001a, 2001b; Gerhardt et al., 2001; Streetman & Banerjee, 2000; Taya, 2005; von Hippel, 1954).

Many additional perspectives and models for electrical response are available in the literature and cannot be reviewed thoroughly here (Balberg et al., 2004; Bertram & Gerhardt, 2009, 2010; Connor et al., 1998; Gerhardt & Ruh, 2001; Lagarkov & Sarychev, 1996; Mebane & Gerhardt, 2006; Mebane et al., 2006; Panteny et al., 2005; Runyan et al., 2001a, 2001b; Tsangaris et al., 1996; C. A. Wang et al., 1998; Zhang et al., 1992). Most of these models adopt a single perspective for considering the structure. In one type, the composite itself is considered as an electrical circuit consisting of a large number of passive elements, such as resistors and capacitors, which are themselves models of individual microstructural features (e.g. SiC_w/matrix/SiC_w structures) and the associated electrical processes. Models of this type are sometimes called equivalent circuits or random-resistor networks (Panteny et al., 2005) Analysis of a random network of passive elements typically starts with basic principles of circuit analysis. Such analyses have provided insight into the electrical response of the systems in question (Bertram & Gerhardt, 2010; Mebane & Gerhardt, 2006).

The filler material may be accounted for in other ways as well. One model took into account both the percolation of the filler particles and the fractal nature of filler distribution in non-

whisker particulate composites and related it to the ac and dc electrical response (Connor et al., 1998). The Maxwell-Wagner model (Bertram & Gerhardt, 2010; Gerhardt & Ruh, 2001; Metaxas & Meredith, 1983; Runyan et al., 2001b; Sillars, 1937; Tsangaris et al., 1996; von Hippel, 1954) originally considered the frequency-dependent ac electrical response of a simple layered composite structure (von Hippel, 1954) based on polarization at the interface of the two phases. Generally, it was found that this model gave similar but not identical results to the Debye model (von Hippel, 1954) for a general dipole polarization. The Maxwell-Wagner model has been extended to consider more complicated geometries for the filler distribution (Sillars, 1937). Recent studies (Bertram & Gerhardt, 2010; Runyan et al., 2001b) have revealed that the Cole-Cole modification (Cole & Cole, 1941) of the Debye model can be applied to describe non-idealities observed experimentally for the Maxwell-Wagner polarizations in SiC-loaded ceramic composites. Unfortunately, there do not seem to be many composite models which account for the semiconductive (Streetman & Banerjee, 2000) character of SiC whiskers. Our description of Schottky-barrier blocking between metal (electrode) and semiconductor (SiC) junctions at whiskers on Al_2O_3-SiC_w composite surfaces is an exception (Bertram & Gerhardt, 2009). The interested reader may also consult other works concerning modeling transport in systems that may be relevant to Al_2O_3-SiC_w but which will not be described here (Calame et al., 2001; Goncharenko, 2003).

3.4. Percolation of General Stick-filled Composites

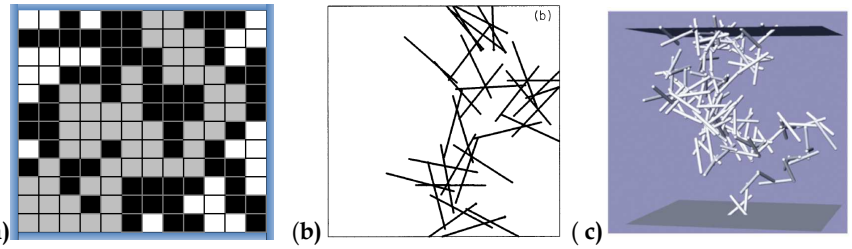

Fig. 4. Top-to-bottom percolation pathways in models of increasing complexity: (a) Binary black-and-white composite on a square grid, where white-percolation is darkened to gray. (b) Two-dimensional stick percolation, (c) Three-dimensional model based on stereological measurements of the length-radii-orientation distribution of SiC whiskers.

Sources: (b) Lagarkov & Sarychev's Fig 1b, *Phys. Rev. B*. 53 (10) 6318, 1996. Copyright 1996 by the American Physical Society. (c) Mebane & Gerhardt, 2006. John Wiley & Sons, with permission.

The fundamentals of the old statistical physics problem of percolation are discussed elsewhere (Stauffer & Aharony, 1994). In Figure 4, it is shown that the percolation transition in composites may be understood on various levels of conceptual complexity. As complexity increases to more accurately describe the stick morphology of the filler, the model changes from (a) a two-dimensional binary pixel array to (b) one-dimensional (1D) rods in 2D space, to (c) 2D rods in 3D space. Electrically, percolation amounts to an insulator-conductor transition (Gerhardt et al., 2001). Percolation also causes a significant change in creep response (de Arellano-Lopez et al., 1998) and hinders densification during composite sintering (Holm & Cima, 1989).

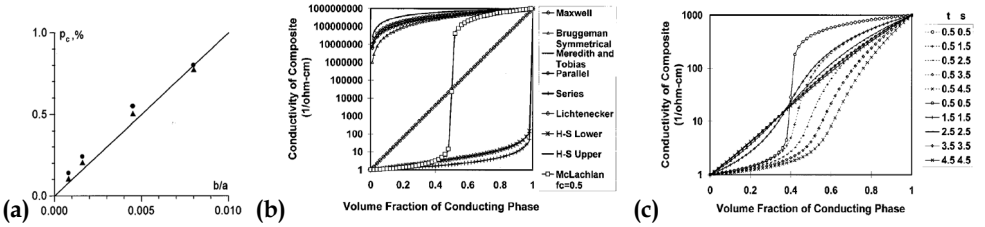

Fig. 5. (a) Linear dependence of percolation threshold (ϕ_c=p_c) on inverse aspect ratio (b/a). (b) Comparison between the McLachlan model of percolation vs. various other models for electric composites. (c) Effect of McLachlan parameters on the shape of the percolation curve when p_c=0.4. *Sources:* (a) Lagarkov et al., 1998. American Institute of Physics. (b-c) Runyan et al, (2001a). John Wiley & Sons.

The actual value of the percolation threshold depends on the shape of the percolating particles, the dimensionality of the structure, the definition of connectivity, and for real composites, the details of processing. In Figure 4a, it is easy to imagine that percolation of white pixels along a particular direction could be achieved with the lowest possible ratio of white-to-black in the overall grid if the white pixels are arranged in a straight line along the direction of interest. This fact relates to the percolation of sticks in 3D space. For sticks having lengths 'a' and diameters 'b', the stick aspect ratio is a/b and is related to the percolation threshold ϕ_c=p_c via

$$p_c \propto b/a \tag{7}$$

Figure 5a demonstrates this with experimental data from chopped-fiber composites (Lagarkov et al., 1998; Lagarkov & Sarychev, 1996). This relation has been concluded by several investigators, can be proven with an excluded volume concept (Balberg et al., 1984; Mebane & Gerhardt, 2006), and has important implications for real composite materials. Generally speaking, simulated and experimental results for percolation thresholds indicate that the percolation process is strongly dependent on the geometric features of the problem and that analytical and computer models are often useful for understanding of specific situations.

The Generalized Effective Medium (GEM) equation first proposed by McLachlan provides a useful model of the percolation transition for general insulator-conductor composites and uses semi-empirical exponents to account for variation in the shapes observed for experimental percolation curves (McLachlan, 1998; Runyan et al., 2001a; Wu & McLachlan, 1998). It may be written as

$$(v_i)\frac{\sigma_i^{1/s}-\sigma_M^{1/s}}{\sigma_i^{1/s}+\left(\frac{1}{\phi_c}-1\right)\sigma_M^{1/s}}+(v_c)\frac{\sigma_c^{1/t}-\sigma_M^{1/t}}{\sigma_c^{1/t}+\left(\frac{1}{\phi_c}-1\right)\sigma_M^{1/t}}=0 \tag{8}$$

where ϕ_c =p_c is the (critical) percolation threshold, σ is dc electrical conductivity, σ_c refers to the conductive phase, ν indicates volume fraction, *s* and *t* are semi-empirical exponents,'M'

denotes the composite mixture, and 'i' denotes the insulator. The McLachlan equation predicts a drastically different response compared to many other composite models, as shown in Figure 5b. Figure 5c shows some effects of the semi-empirical parameters on the shape of the percolation curve. The percolation of rods having specific size and orientation distributions has been simulated (Mebane & Gerhardt, 2006) and this model required certain assumptions about the nature of interrod connectivity, e.g. a "shorting distance" concept.

3.5. Structural Characteristics of Al_2O_3-SiC_w Composites

What should one focus on when considering the complicated microstructure of a Al_2O_3-SiC_w composite? There are many options, including density, whisker size and orientation, whisker percolation, interwhisker distance, whisker-matrix interface properties, and whisker defects. Many of these will be considered in this section, and a discussion of interface effects and SiC_w defects is given in Section 3.8. Properties of the Al_2O_3 and sintering additives seem to have less impact on the final properties (assuming high density is achieved) and will not be considered here.

3.5.1. Percolation of SiC Whiskers

The formation of a continuous percolated network of SiC whiskers across a sample has important implications for electrical/thermal transport and mechanical properties (de Arellano-Lopez et al., 1998, 2000; Gerhardt et al., 2001; Holm & Cima, 1989; Mebane & Gerhardt, 2004, 2006; Quan et al., 2005). For hot-pressed ceramic composites, it seems that percolation tends to occur in the 7 to 10 vol% range. One study, which considered creep response, associated these lower and upper bounds with point-contact percolation and facet-contact percolation respectively (de Arellano-Lopez et al., 1998). This range is also consistent with experimental data for electrical percolation (Bertram & Gerhardt, 2010; Mebane & Gerhardt, 2006). Most work investigating percolation is based on electrical response because it is (arguably) much easier to perform the needed experiments compared to those for mechanical response. Electrically, the SiC_w are at least ~9 orders of magnitude more conductive than Al_2O_3. Thus, they are likely to carry much more current than the matrix and the majority of the current through the sample. Therefore, the percolation of the SiC_w is of principal importance in the determination of the composite electrical properties. Composites having such contrast in conductivity between the filler and the matrix undergo a drastic change in electrical response when the conductive filler becomes interconnected within the sample such that a continuous pathway of filler spans the sample. However, percolation is also known to affect mechanical (creep) response (see Section 3.6.2.) and reduce sinterability of composites due to the formation of a rigid interlocking network (Holm & Cima, 1989).

Consideration of this fact raises a question: for a dispersed binary composite (e.g. Al_2O_3-SiC_w), does the percolation threshold depend on the property or process of interest? This question can be reframed in terms of (1) mechanical percolation vs. electrical percolation, or (2) general percolation theory in regards to how one defines a "connection" between two squares on the black-and-white grid of Figure 4a. For electrical percolation in composites of dispersed particles that are much more conductive than the matrix, the prevailing theories(Balberg et al., 2004; Connor et al., 1998; Sheng et al., 1978) generally propose that

direct physical contact between the particles is *not* required, and that charge transport takes place by tunneling or hopping across interfiller gaps. Thus, for electrical considerations, one may consider two whiskers to be connected even if they are separated by physical space. For mechanical percolation, the underlying concept of a rigid percolated network implies intimate physical contact between SiC_w spanning the entire sample and that electrical percolation could exist without mechanical percolation. If true, electrical and mechanical percolation thresholds for Al_2O_3-SiC_w and similar composites need not coincide. In order to verify such a difference, a study investigating electrical and mechanical percolation on the same set of samples is required.

3.5.2. Properties of the Spatially Dispersed SiC-Whisker Population

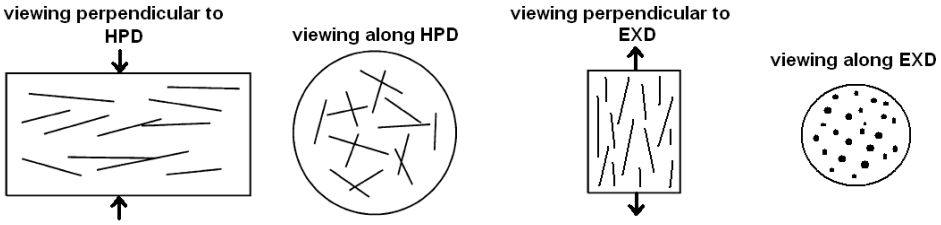

Fig. 6. Schematics showing the preferred orientations of SiC whiskers which result from the hot-pressing and extrusion-based processing methods. The processing directions (HPD and EXD, respectively) are marked by arrows. HP figures after Mebane and Gerhardt, 2006 (John Wiley & Sons).

The whisker sizes and orientations generally affect the properties of interest for the composite applications and so the Al_2O_3-SiC_w structure has often been discussed as such. The ball-milling process often used for mixing the component powders seems to result in a lognormal distribution of whisker lengths peaking around ~10 μm (Farkash & Brandon, 1994; Mebane & Gerhardt, 2006). The preferred whisker orientation depends on the fabrication method. In hot-pressed composites, whiskers tend to be aligned perpendicular to the hot-pressing direction (HPD) and have random orientation in planes perpendicular to the HPD (Park et al., 1994; Sandlin et al., 1992). In extruded samples, the whiskers are expected to be approximately aligned with the extrusion direction (EXD). These preferred orientations are shown in Figure 6. Such material texture generally results in anisotropy in both electrical and mechanical properties and has been shown for hot-pressed samples (Becher & Wei, 1984; Gerhardt & Ruh, 2001).

In consideration of the SiC_w dispersion as the most important aspect of the microstructure, one can characterize the associated trivariate length-radii-orientation distribution with a comprehensive stereological method (Mebane et al., 2006). Other methods also exist for determining the orientation distributions of SiC_w or estimating the overall degree of preferred alignment (texture) and generally result in a unitless orientation factor between 0 and 1. One measurement based on x-ray-diffraction-based texture analysis was effectively correlated to the composite resistivity (C. A. Wang et al., 1998). Another orientation factor

based on a different stereological method increased linearly with the length/diameter ratio of the extrusion needle, and thus seemed effective (Farkash & Brandon, 1994). However, for both of these methods, information about the coupling of whisker size and orientation distributions which is known to exist (Mebane et al., 2006) is lost.

3.5.3. Microstructural Axisymmetry

The preferred orientation of SiC_w in hot-pressed and extruded samples has been studied by multiple investigators (Park et al., 1994; Sandlin et al., 1992) and means that the composites tend to be symmetrical around the processing direction (e.g. the HPD or EXD). In other words, both hot-pressed and extruded samples possess a single symmetry axis in regards to the SiC_w distribution and therefore have axisymmetric microstructures. Such composite materials can be considered to have only two principal directions in terms of property anisotropy: (1) the processing direction, and (2) the set of all directions which are perpendicular to the processing direction and are therefore equivalent.

Fig 7. Scanning electron micrographs of the microstructure for an Al_2O_3-SiC_w sample containing 14.5 vol% SiC_w. In (a), the white arrow points along the hot-pressing direction. In (b), the microstructure is viewed along this direction. Part (c) shows the average distance between SiC inclusions along the HPD and perpendicular direction. The inset shows a schematic of the microstructure. *Source:* Bertram & Gerhardt, 2010.

Recently, a simple but useful stereological characterization method was developed and applied to Al_2O_3-SiC_w composite microstructures like those shown in Figures 7a and 7b (Bertram & Gerhardt, 2010). In this method, the distributions of distances between the SiC phase are characterized with stereological test lines as a function of principal direction in the microstructure. We propose that the results implicitly contain information about whisker sizes, orientations, dispersion uniformity and agglomeration and should be generally relevant for transport properties dominated by the SiC phase. For example, anisotropy in average interparticle distance (Fig. 7c) was strongly correlated to electrical-resistivity anisotropy (not shown).

3.5.4. Performance-based Perspective on Composite Structure

For complicated materials such as dispersed-rod composites, it is especially important to remember that structure determines properties and properties determine performance. To meet performance specifications for an application, certain properties must be optimized. After mixing component powders, Al_2O_3-SiC_w composites are usually consolidated and solidified by dry-pressing followed by hot-pressing or extrusion followed by pressureless-sintering. For these materials, the cutting and microwave-heating applications imply that

the process engineer often desires the following structural characteristics for the final ceramic:

- a density as close to theoretical as possible (porosity has deleterious effects on properties)
- uniform whisker dispersion (for better toughness, strength, conductivity)
- minimal whisker content to minimize cost while achieving the desired properties
- percolation, for conductive electrical response and improved mechanical response
- "medium" whisker aspect ratios (e.g. 10<length/width<20) to balance the needs for percolation and high sintered density
- no particulate SiC, only whiskers (SiC particulates do not improve properties as much)
- silica- and glass-free (clean) interfaces between the whiskers and the matrix (for toughness)
- a ceramic matrix material that is both inexpensive and environmentally friendly

3.6 Selected Mechanical, Thermal, and Chemical Behavior

3.6.1 Effects of SiC Whiskers on Mechanical Properties and Deformation Processes

Inclusion of SiC whiskers in a ceramic matrix generally increases the material strength but is mainly done to reduce the brittle character of the ceramic. Failure of brittle materials usually results from crack growth, a process driven by the release of elastic stress-strain energy of the atomic network (e.g. the crystal or glass) and retarded by the need to produce additional surface energy (Richerson, 1992). The whiskers tend to increase the fracture toughness and work of fracture by redirecting crack paths and diverting the strain energy which enables crack growth. Toughening mechanisms include modulus transfer, crack deflection, crack bridging, and whisker pull-out. Some examples of these are shown in Figure 8.

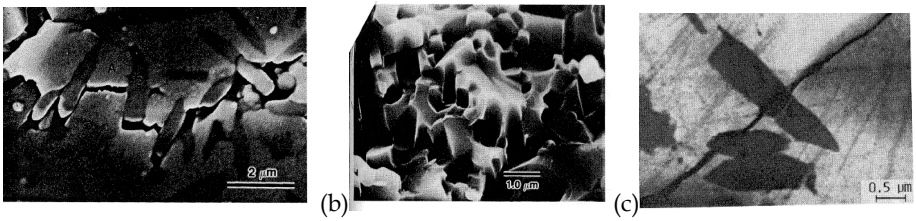

Fig 8. Examples of whisker toughening mechanisms: (a) crack deflection, (b) whisker pull-out, (c) crack bridging. *Sources:* (a) J. Homeny et al., 1990. John Wiley & Sons (b) F. Ye et al., 2000. Elsevier. (c) R.H. Dauskardt et al., 1992. John Wiley & Sons.

In modulus transfer, the stress on the matrix is transferred to the stiffer and stronger whiskers. In crack deflection, cracks are forced to propagate around whiskers due to their high strength, effectively debonding them from the matrix and creating new free surfaces. In crack bridging, whiskers which span the wakes of cracks impart a closing force, absorbing some of the stress-strain energy (concentrated at the crack tip) and thereby reducing the impetus for crack advancement. Some bridging whiskers debond from the matrix or rupture, resulting in pull-out. The associated breakage of interatomic bonds and frictional sliding also increase the work of fracture.

One study (Iio et al., 1989) showed that the inclusion of SiC whiskers up to 40 vol% increased the fracture toughness of pure alumina from ~3.5 up to ~8 MPa·$m^{1/2}$ for samples hot-pressed at 1850°C. However, such large gains only apply when the crack plane is parallel to the hot-pressing direction. This orientation provides for more interactions between the whiskers and the crack in comparison to when the crack plane is perpendicular to the hot-pressing direction. In the latter situation, the cracks can avoid the whiskers more easily and only modest improvements in toughness are achieved. It was also found that the fracture strength increases from ~400 MPa to ~720 MPa in going from 0% to 30 vol% SiC_w and decreased as whisker content increased to 40 vol%. The improvement is the result of the increased likelihood of whisker-crack interactions when whisker content is increased. They found that changing the hot-pressing temperature to 1900°C, despite improving densification, significantly reduced the toughness for 40 vol% samples and correlated this to a reduction in crack deflections and load-displacement curves being characteristic of brittle failure with no post-yield plasticity (unlike samples pressed at 1850°C). Scanning and transmission electron microscopy revealed different whisker-matrix interfacial structure for the different temperatures and suggested that matrix grain growth at 1900°C led to whisker agglomerations (Iio et al., 1989). The authors concluded that the distribution of SiC whiskers is of principal importance in determining the strength and toughness of the material and that whisker agglomerations may act as stress concentrators adversely affecting toughening mechanisms and initiating failure. From the 1850°C pressing temperature, analysis revealed failure initiating at clusters of micropores from incomplete densification.

Modeling work indicates that whisker bridging in the wake of the crack tip is the most important toughening contribution(Becher et al., 1988, 1989). Two different modeling approaches (stress intensity and energy-change) were used to determine the following relationship between the bridging-based toughness improvement (dK_{Ic}) imparted to the composite from the whiskers and several parameters:

$$dK_{Ic} = \sigma_{w,f}\left(\frac{V_w r_w}{6(1-\nu^2)}\frac{E_c}{E_w}\frac{G_m}{G_i}\right)^{\frac{1}{2}} \tag{9}$$

Here, r_w V_w and E_w are the radius, volume fraction and elastic modulus of the whiskers, respectively. The whisker strength at fracture is $\sigma_{w,f}$. The Poisson ratio and elastic modulus of the composite are ν and E_c, respectively. Strain-energy release rates are given by G, where subscripts indicate the matrix (m) and the whisker-matrix interfaces (i).

3.6.2. Creep Response and High-Temperature Chemical Instability

Prolonged high-temperature exposure to mechanical stress leads to creep, degradation of Al_2O_3-SiC_w composite microstructures, and worsening of mechanical properties. Creep in these composites has been studied at temperatures from 1000°C to 1600°C and resistance to creep is generally much better than that of monolithic alumina (Tai & Mocellin, 1999). Figure 9a shows that, for a given stress level, the creep strain rate at 1300°C is much reduced if whisker content is increased. However, stressing for long times at elevated temperature has resulted in composite failure well-below the normal failure stress at a given

temperature. For example, one study found failure occurring at 38% of the normal value after stressing in flexure for 250 hours at 1200°C (Becher et al., 1990).

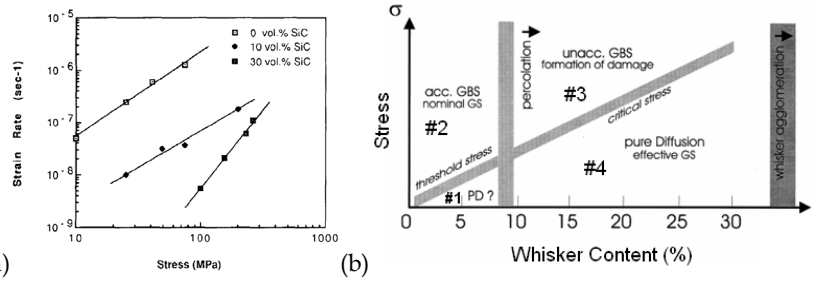

Fig. 9. (a) Effect of whisker content on stress-strain relations during compressive creep at 1300°C. (b) Creep deformation mechanism map showing the effects of stress and whisker content on the dominant deformation mechanism. *Sources:* (a) Nutt & Lipetzky, 1993. (b) De Arellano-Lopez et al., 1998 (region numbers added). From Elsevier, with permission.

Creep in polycrystalline ceramics often proceeds by grain boundary sliding (Richerson, 1992). Due to rigid particles (whiskers) acting as hard pinning objects against grain boundary surfaces, such sliding is impeded in alumina-SiC_w composites and creep resistance is improved (Tai & Mocellin, 1999). For such systems, one model (Lin et al., 1996; Raj & Ashby, 1971) predicts the steady state creep strain rate ($\dot{\varepsilon}$) to be

$$\dot{\varepsilon} = C\frac{\sigma_a{}^n}{d^u r_w^q V_w}\exp\left(-\frac{Q}{RT}\right) \tag{10}$$

where C is a constant, σ_a is the applied stress, d is the grain size, r_w is the whisker radius, V_w is the whisker volume fraction, Q is the apparent activation energy, R is the gas constant, and T is the absolute temperature. The exponents n, u, and q are phenomenological constants. The stress exponent n is of particular interest because it has been correlated to the dominant deformation mechanism (de Arellano-Lopez et al., 2001; Lin et al., 1996; Lin & Becher, 1991).

The qualitative dependence of deformation mechanism on stress, temperature, and whisker content is best understood by considering the deformation map of Figure 9b, which was developed after many years of research on the creep response (de Arellano-Lopez et al., 1998). The applicability of this map does not seem to depend on whether or not creep is conducted in flexure or compression. In region #1, the dominant mechanism is Liftshitz grain boundary sliding, which is also called pure diffusional creep (PD) in the literature. In this process, grains elongate along the tensile axis and retain their original neighbors. Above the threshold stress, which relates to whisker pinning, Rachinger grain boundary sliding (GBS) becomes the dominant mechanism (region #2). In this process, grains retain their basic shapes and reposition such that the number of grains along the tensile axis increases. Grain rotation has been observed in some cases (Lin et al., 1996; Lin & Becher, 1990). Both the Liftshitz and Rachinger processes are accommodated by diffusion that is believed to be rate-limited by that of Al^{3+} ions through grain boundaries (Tai & Mocellin, 1999).

When whisker content exceeds the percolation threshold, the creep rate does not depend on the nominal alumina grain size but rather on an effective grain size which is defined by the volumes between whiskers (de Arellano-Lopez et al., 2001; Lin et al., 1996). The percolated whisker network provides increased resistance to GBS and this relates to the critical stress, below which deformation proceeds by PD (region #4). Increasing the stress above this critical value marks a transition to grain boundary sliding that can no longer be accommodated by diffusional flow and requires the formation of damage (region #3). Both the critical and threshold stress decrease with increasing temperature. Also, one should note that the boundaries between the different regions are not strict. For example, Rachinger sliding has occurred in samples having whisker fractions as high as 10 vol% (de Arellano-Lopez et al., 2001).

In region #3, whiskers seem to promote damage such as cavitation, cracking, and increased amounts of silica-rich glassy phases at internal boundaries and cavities (de Arellano-Lopez et al, 1990; Lin & Becher, 1991). Examples of such damage are shown in Figures 10a-b. The cavitation and cracking is believed to be result of whiskers acting as stress concentrators and the presence of glass pockets is from the thermal oxidation of whiskers (de Arellano-López et al., 1993). High stress results in less grain-boundary sliding and promotes cracking, separation of matrix grains from whiskers, and the formation of cavities within glass pockets at whisker/whisker and whisker/matrix interfaces (Lipetzky et al., 1991). Whisker clusters containing cavitation and crack growth have also been reported for higher (≥25 vol%) loadings of SiC_w (O'Meara et al., 1996).

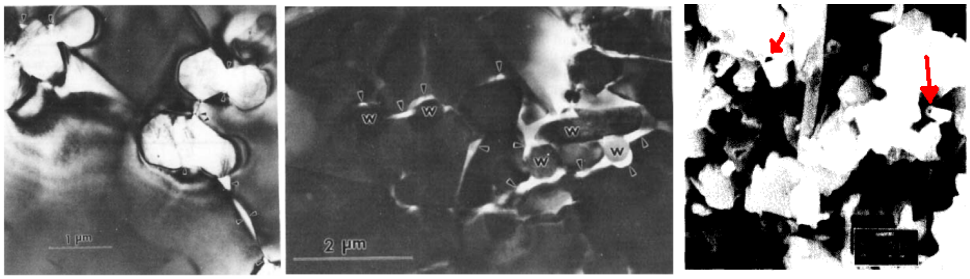

Fig. 10. (a) TEM of glass-filled cavities which formed near SiC_w in a 20 vol% SiC_w composite during creep (b) TEM of cavitation and cracking near whiskers (w) during creep (c) Whisker hollowing (red arrows) on a fracture surface from the bulk after annealing in air at 1000°C for 1 hr. *Sources*: (a-b) de Arellano-Lopez et al., 1993. John Wiley & Sons (c) S. Karunanithy, 1989 (arrows added). From Elsevier, with permission.

The ion diffusion that assists grain boundary sliding is believed to be accelerated by the presence of intergranular glassy regions and further complemented by the viscous flow of this glass. The amount of glassy phase in as-fabricated composites is generally small but increases in size after creep deformation in air ambient due to oxidation of SiC whiskers, resulting in a SiO_2-rich glassy phase surrounding the whiskers. Such whisker oxidation has been observed to occur in the bulk of samples and is attributed to residual oxygen on whisker surfaces, enhanced oxygen diffusion through already-formed glass, and short-circuit transport through microcracks. Also, much of the glass found in the bulk is believed

to originate from oxidation scales on the composite surfaces flowing into internal interfaces. During creep, the glassy phase apparently seeps into grain boundaries, interfaces, and triple grain junctions (de Arellano-Lopez et al., 1990; Lin et al., 1996; Lin & Becher, 1991; Nutt, 1990; Tai & Mocellin, 1999).

It is believed that glass formation begins with the oxidation of SiC. This yields silica and/or volatile silicon monoxide products which subsequently react with alumina to produce aluminosilicate glass. This glass has been observed to contain small precipitates of crystalline mullite and is believed to accelerate oxygen diffusion compared to pure silica glass. Such an acceleration might explain the overall fast oxidation rate of the composite, which exceeds that of pure SiC by more than an order of magnitude (Jakus & Nair, 1990; Karunanithy, 1989; Luthra & Park, 1990; Nutt et al., 1990). The following reactions can account for these transformations:

$$SiC(s) + 3/2\ O_2(g) \rightarrow SiO_2(l) + CO(g) \quad (11)$$

$$SiC(s) + O_2(g) \rightarrow SiO(g) + CO(g) \quad (12)$$

$$2SiC(s) + 3Al_2O_3(s) + 3O_2(g) \rightarrow 3Al_2O_3 \cdot 2SiO_2(s) + 2CO(g) \quad (13)$$

$$SiC(s) + O_2(g) \rightarrow SiO_2(l) + C(s) \quad (14)$$

As indicated above, the presence of oxygen in the atmosphere affects creep and results in higher creep rates compared to inert gas. Another process that may make use of oxygen was observed after heat treatment in air at 1000°C: whisker-core hollowing. Core hole diameters ranged from 200 to 500 nm and were attributed to metallic impurities and the decomposition of oxycarbide in whisker-core cavities that are known to exist in as-fabricated whiskers. The core-hollowing phenomenon was seen on fracture surfaces after breaking heat-treated samples with a hammer, suggesting its occurrence throughout the bulk of the sample. Such a fracture surface is shown in Figure 10c (Karunanithy, 1989).

Generally, the oxidation occurring on the composite surface as a result of the ambient has been found to depend on the partial pressure of the oxidizing agent. In most studies, molecular oxygen is the oxidizing agent of interest. When the oxygen partial pressure is low, active oxidation occurs and Reaction 12 is operable: SiC is lost into the gas phase. Otherwise, passive oxidation occurs in the form of Reaction 14, which results in free carbon and liquid SiO_2, which then mixes with alumina to form aluminosilicate glass, from which mullite often precipitates. When passive oxidation occurs, this can result in surface scales and crack blunting/healing which can mitigate the degradation of mechanical properties (Shimoo et al., 2002; Takahashi et al., 2003). Another study (Kim & Moorhead, 1994) showed that the oxidation of SiC at 1400°C may significantly increase or decrease the strength depending on the partial pressure of oxygen.

In air at 1300-1500°C, (Wang & Lopez, 1994) oxidation results in the formation of layered scales, consisting of a porous external layer on top of a thin ($0 < 6$ μm) layer of partially oxidized SiC_w and glassy phases. Intergranular cracking occurred in this thin layer and was attributed to volume changes associated with the oxidation reaction. The rates of scale-thickening and weight gain were parabolic and rate constants and activation energies were calculated and ascribed to diffusion of oxidant across the porous region. At 600-800°C, oxidation obeys a linear rate law for

the first 10 nm of oxide growth (P. Wang, et al., 1991). From 1100-1450°C, oxidation has also been found to degrade the elastic modulus of samples. It has also been found that the presence of nitrogen in the ambient at elevated temperatures may similarly result in the chemical degradation of the SiC_w and composite properties (Peng et al., 2000).

3.6.3 Thermal Conductivity

Thermal conductivities of hot-pressed Al_2O_3-SiC_w composites along the hot-pressing direction typically range from ~35-50 W/m·K for 20-30 vol% composites at 300 K and the highest ever reported was 49.5 W/m·K (Collin & Rowcliffe, 2001; Fabbri et al., 1994; McCluskey et al., 1990). Such volume fractions of whiskers likely translate to SiC_w percolation, but the associated thermal conductivity values are not much higher than those of the Al_2O_3 (~30 W/m·K). This can be understood in terms of modeling results for conductive nanowire composites which show that percolation does not lead to a dramatic increase in thermal conductivity because of phonon-interface scattering (Tian & Yang, 2007). In an experimental study of Al_2O_3-SiC_w composites, it was estimated that the SiC_w phase has a thermal conductivity that is 90-95% lower than that of ideal cubic SiC based on a model for overall composite thermal conductivity and planar defects spaced 20 nm apart in the SiC_w could account for this discrepancy (McCluskey et al., 1990). Such a spacing agrees well with stacking fault densities observed in the whiskers (Nutt, 1984). It has also been found that the preferred orientation of the SiC_w results in the composites having significant anisotropy in thermal diffusivity and conductivity (Russell et al., 1987).

3.6.4 Cycling Fatigue from Thermal Shock

In ceramic matrix composites, fatigue during thermal shock cycling is believed to be the result of the thermal-gradient imposed stresses and thermal expansion mismatch between the two phases. The addition of silicon carbide whiskers results in significant improvements in thermal shock resistance compared to monolithic alumina. One study found that a thermal shock quench with a temperature difference of 700°C caused a 61% decrease in flexural strength for pure alumina (Tiegs & Becher, 1987). For samples having 20 vol% SiC_w, the strength loss after ten similar quenches was only 13% of the original value. The improvement is generally attributed to whiskers toughening effects on shock-induced microcracks. A reduction in thermal gradient due to an increase in composite thermal conductivity provided by the whiskers is also believed to contribute to the improved thermal shock resistance but is expected to be of less importance (Collin & Rowcliffe, 2001).

Another study (Lee & Case, 1989) found that the amount of thermal shock damage saturates as a function of the number of increasing thermal shock cycles and that the saturation value depends strongly on the shock temperature difference, ΔT. This is shown in Figure 11, which displays the effects of these factors on elastic modulus. Since crack density is expected to vary inversely with the elastic modulus (Budiansky & Oconnell, 1976; Salganik, 1973), Figure 11 suggests that ΔT is more important than the number of cycles in determining the extent of damage.

The modulus values were obtained by the sonic resonance method (Richerson, 1992) which is sensitive to the distribution of cracks in each sample. This method allowed for a reduction

in sample size in comparison to that needed for measurements based on the stochastic process of brittle fracture. It was possible to reuse samples by annealing out damage at 950°C and near-full recovery of elastic properties was achieved (Lee & Case, 1989). However, only samples with 20 vol% whisker loading were investigated in this work.

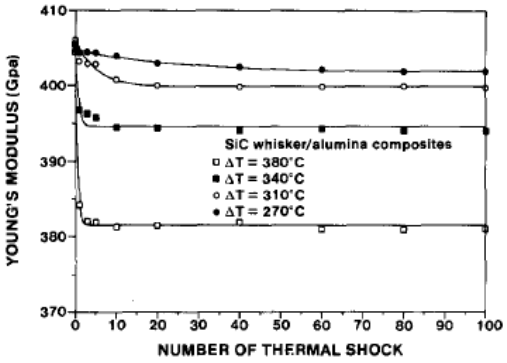

Fig. 11. Dependence of composite elastic modulus on thermal-shock quenching temperature difference, ΔT, and the number of quenches performed. *Source:* Lee & Case, 1989. Elsevier.

In contrast to the thermal-shock work on hot-pressed composites discussed above, composites made by extrusion and sintering were reported to withstand shocks of almost 500°C and lost only 12% of strength after 400 shocks of 230°C. Strength slowly decreased with cycling and did not plateau (Quantrille, 2007).

3.7. Electrical Response

3.7.1. Relevant Formalisms

In general, complex relative dielectric constant ε_r^* of a material is composed of a frequency-dependent real part ε_r' (the dielectric constant) and imaginary part $j\varepsilon_r''$ and may be written as

$$\varepsilon_r^* = \varepsilon_r' - j\varepsilon_r'' \tag{15}$$

where $-\varepsilon_r''$ is the dielectric loss, $j = \sqrt{-1}$ and the subscript "r" indicates relation to the vacuum permittivity ε_0, i.e. the complex permittivity of a general medium is $\varepsilon^* = \varepsilon_0\varepsilon_r^*$. The complex permittivity is related to the complex impedance ($Z^*=Z'-jZ''$) via

$$Z^* = 1/j\omega C_0\varepsilon_r^* \tag{16}$$

where ω is the radial frequency and C_0 is the geometric capacitance. The real impedance (Z') may be converted to resistivity or conductivity after geometric normalization. The volumetric microwave-heating rate of a material at a particular frequency depends mainly on the dielectric loss and is given by

$$\left(\frac{dT}{dt}\right)_V = \frac{2\pi f E^2\left(-\varepsilon_r''\right)\varepsilon_0}{DC_p} \tag{17}$$

where f is the frequency, E is the magnitude of electric field, C_p is the heat capacity at constant pressure, and D is the material density (Bertram & Gerhardt, 2010; Metaxas & Meredith, 1983). Thus, $-\varepsilon_r''$ is the material property that determines the power delivered per unit volume (i.e. the numerator in Equation 17) and generally includes loss contributions from all forms of frequency-dependent polarization or resonance and the dc conductivity σ_{dc} of the material, i.e.

$$(-\varepsilon_r'') = (-\varepsilon_r'')^{di} + (-\varepsilon_r'')^{ion} + (-\varepsilon_r'')^{el} + (-\varepsilon_r'')^{MW} + \frac{\sigma_{dc}}{2\pi f \varepsilon_0} \quad 18)$$

Here, the superscripts refer to dipolar (di), ionic (ion), electronic (el) and Maxwell-Wagner (MW) polarizations and the last term in the sum follows from the Maxwell-Wagner theory of a two-layer condenser (Metaxas & Meredith, 1983; von Hippel, 1954). The complex dielectric constant resulting from a Maxwell-Wagner interfacial space-charge polarization $(\varepsilon_r^*)^{MW}$ can be written as

$$(\varepsilon_r^*)^{MW} = \varepsilon_\infty' + \frac{\varepsilon_s' - \varepsilon_\infty'}{1 + (j\omega\tau)^{1-\alpha}} - j\frac{\sigma_{dc}}{\omega\varepsilon_0} \quad (19)$$

where ε_∞' and ε_s' are the real parts of the complex relative dielectric constant at the high- and low-frequency extremes, $\omega=2\pi f$, τ is the characteristic relaxation time, and $(1-\alpha)$ is an empirical fitting exponent which accounts for a distribution of relaxation times (Bertram & Gerhardt, 2010; Runyan et al., 2001b). For an ideal Maxwell-Wagner polarization with a single relaxation time, $\alpha=0$. The explicit effects of α on the real and imaginary parts of ε_r^* were determined more than 60 years ago (Cole & Cole, 1941). It is also common to apply an empirical exponent (k) to the frequency (ω) of the $j\sigma_{dc}/\omega\varepsilon_0$ term of Equation 19 to better fit the low-frequency part of the loss spectrum.

The standard frequencies for microwave oven operation are 2.45 and 0.915 GHz. At these frequencies, loss-based heating in the composites will occur preferentially in the SiC_w phase compared to Al_2O_3 due to much greater values of $-\varepsilon_r''$. One study found that loss values are ~180 times greater for SiC compared to Al_2O_3 (Basak & Priya, 2005). However, the dielectric properties of SiC are known to vary widely depending on the crystalline structure and impurity content. Notably, the SiC_w made by Advanced Composite Materials LLC are known to be exceptionally lossy (Quantrille, 2007).

3.7.2. Preliminary Work on SiC_w Composites

In 1992, it was found that the resistance of the composite decreased linearly with temperature. This was attributed to the semiconductive nature of SiC (Zhang et al., 1992). On a similar system, for which the matrix was mullite instead of alumina, the dc conductivity and frequency-dispersions of the dielectric constant depended on measurement orientation relative to preferred orientation of whiskers (Gerhardt & Ruh, 2001). This paper also showed the effect of volume fraction on dielectric-property spectra of the composites in the 10^2-10^7 Hz frequency range. Later, the orientation dependence was confirmed for the Al_2O_3-SiC_w system (Mebane & Gerhardt, 2004). Both studies noted that representative impedance spectra contain two semicircles in the complex impedance plane and that dc conductivity increased with whisker volume fraction.

In another work, SiC_w composite properties were measured in the 2-18 GHz range with a coaxial airline system (Ruh & Chizever, 1998). Adding ~30 vol% SiC_w to mullite greatly increased the dielectric loss from ~0.0-0.2 up to 6-10 and the dielectric constant increased by 2-3 times. Adding 32.4 vol% SiC_w to a spinel matrix increased the loss from ~0 to 13-20 and increased the dielectric constant by 5-6 times. These results suggest that the matrix can play a significant role in macroscopic electrical response.

3.7.3. Recent Investigations Combining Measurements and Modeling

For composites with SiC_w, multiple interpretations have been proposed for the two complex-impedance semicircles which are generally observed during parallel-plate measurements on percolated samples. Presently, the accepted interpretation of this result is that the higher-frequency semicircle is associated with the bulk conductivity through the whisker network and the lower frequency semicircle relates to blocking processes at the electrodes (Mebane & Gerhardt, 2006). The establishment of these semicircles as being related to specific processes has allowed for modeling of the associated contributions to the electrical response.

3.7.4. Bulk Electrical Response

Recently, the higher-frequency impedance semicircle was considered to be a function of the trivariate length-radius-orientation distribution of the whiskers measured by stereology (Mebane & Gerhardt, 2006). A computer simulation using such distribution information from stereological measurements was used to convert the experimental whisker network in simulation space to a resistor network based on an estimate of $SiC_w/Al_2O_3/SiC_w$ interfacial conductance assuming a tunneling-mechanism-based "shorting distance" for defining interwhisker connectivity. Kirchoff's Laws were then applied to the equivalent circuit generated for different volume fractions of SiC_w. The results were then converted to effective conductivities for the simulated whisker networks and these were compared to the experimental dc-conductivities. It was found that the simulation overpredicted the rate of conductivity-increase with whisker content, which suggests that a conductivity-limiting factor was not accounted for in the simulation. It was also found that the size of the low-frequency impedance semicircle depended on electrode area but not sample thickness, thereby implying that this semicircle was related to the electrodes. In this work, the percolation threshold was experimentally determined to be ~9 vol%.

In another work, the real and imaginary parts of the dielectric response of hot-pressed Al_2O_3-SiC_w were concurrently modeled using a similar formalism (Bertram & Gerhardt, 2010). In this work, ac electrical measurements were conducted over a wide frequency range and indicate that interfiller interactions are probed between ~0.1-1 MHz and ~1 GHz. The response changed from dielectric to conductive across the percolation threshold (5.8-7.7 vol%), as shown in Figure 12a. Non-percolated samples were characterized by a Maxwell-Wagner interfacial polarization with a broad loss peak indicating a distribution of relaxation times and a dc-conductivity tail which was more prominent for samples nearer to the percolation threshold. These features are shown in Figure 12b, along with the real part of the relaxation. Modeling the response based on Equation 19 revealed that the Cole-Cole non-ideality exponent α was larger for the hot-pressing direction. Compared to earlier

investigations, the microstructure of the whisker network was interpreted with a different perspective, i.e. as two distributions of interfiller distances along the two principal directions of the axisymmetric microstructure. The orientation and composition dependencies of the relaxation time were explained in terms of the different average distances for high-frequency capacitive coupling between fillers, i.e. SiC-Al_2O_3-SiC interactions. This distance was found to be shorter along the microstructural symmetry axis (i.e. the HPD) compared to the perpendicular direction, as seen in Figure 7c. But, Figure 12a shows that the resistivity was actually higher along the HPD. The inset of Figure 12a shows the relation between the orientation-based differences in average distance and dc resistivity. This trend could be modeled as cubic or exponential and suggests that the whisker network becomes increasingly isotropic as volume fraction increases.

The relevance of percolation to the composition dependence and the relevance of the Maxwell-Wagner interfacial polarization model for the dielectric response of SiC_w composites has been known for several years (Gerhardt & Ruh, 2001). The frequency dependence of the dielectric constant for a similar system with SiC platelets has also been modeled with a Maxwell-Wagner formalism modified with a Cole-Cole exponent to account for non-ideality in the experimental response (Runyan et al., 2001b).

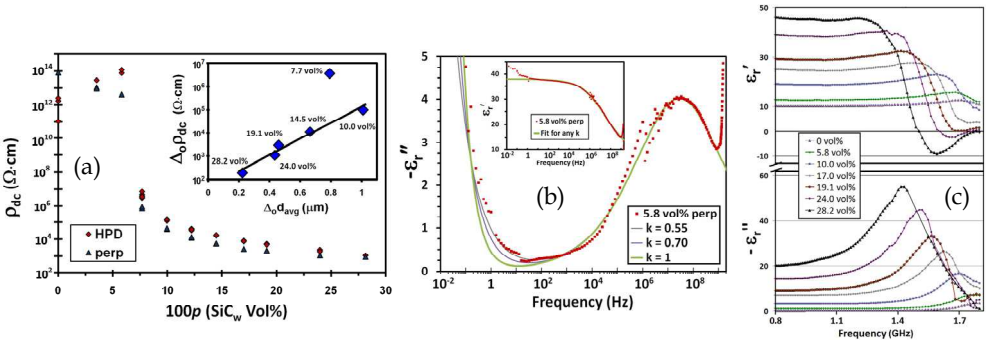

Fig 12. (a) Percolation curves for dc resistivity in the hot-pressing direction (HPD) and perpendicular direction. Inset shows the relation between the direction-based differences in resistivity and inter-SiC distance from Figure 7c. (b) Dielectric loss spectrum of 5.8 vol% SiC_w composite fitted with Equation 19 and various *k* values. (c) Real and imaginary parts of the observed dielectric resonance. All parts a-c from Bertram & Gerhardt, 2010.

The dependence of dc conductivity on SiC_w content for percolated samples fit well to models for fluctuation-induced tunneling theory. The percolation transition from insulating to conducting caused the Maxwell-Wagner dc-conductivity tail to greatly increase in prominence such that it concealed the related dielectric loss peak via superposition (not shown). The frequency-dependent dielectric constant and loss were generally smaller in the HPD compared to the perpendicular direction (not shown).

Also, a damped resonance was observed between 1.4 - 1.7 GHz and was found to shift to lower frequency and increase in magnitude as whisker content increased, as shown in Figure 12c. However, the source of the resonance has not been conclusively established. It

may relate to dopants in the SiC_w, sintering-additive reaction products at grain boundaries, long-range interactions characteristic of conductive-stick composites, or an anomalous instrumental effect. Generally speaking, the commercial application of these composite materials in microwave heating is probably influenced by the resonance, the relaxation, and the dc-conductivity tail. All of these are related to the SiC content.

3.7.5. Electrode/Contact Electrical Response

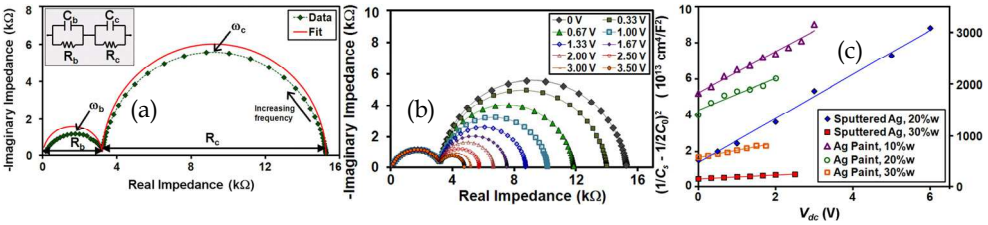

Fig 13. (a) Typical complex impedance data for percolated Al_2O_3-SiC_w material, with a fit based on the equivalent-circuit model in the inset. (b) Effect of dc bias on the complex impedance data. (c) Effect of dc bias on the Mukae capacitance function, revealing the applicability of symmetrical Schottky blocking at the electrodes. *Source:* Bertram & Gerhardt, 2009. Copyright American Institute of Physics.

The electrical response at the electrodes has also been studied in detail (Bertram & Gerhardt, 2009). Electrical contacts to Al_2O_3–SiC_w composites are manifested in the complex impedance plane by a semicircle that is well-modeled by a parallel resistor-capacitor circuit having a characteristic relaxation time. This appears in Figure 13a on the right side, next to the higher-frequency bulk-response semicircle on the left. As dc bias is increased, the bulk response (related to the whisker network) is unaffected and the electrode semicircle shrinks, as shown in Figure 13b. The dc capacitance-voltage data associated with the electrode semicircle evidenced that the underlying physical process was blocking by symmetrical Schottky barriers (at the opposing electrodes). Figure 13c shows this with straight-line fits to the bias-dependent capacitance function derived for symmetrical Schottky blocking (Mukae et al., 1979).

The effect of the bulk electrode material was also studied. Compared to sputtered metal electrodes, samples having silver-paint electrodes had inferior properties, i.e. higher values of area-normalized resistance and lower values of area-normalized capacitance. These differences were attributed to more limited interfacing between metal particles and whiskers on the composite surface for painted samples. Sputtered contacts of Pt were superior to those of Ag, suggesting a dependence on metal work function. Charge carrier concentrations were estimated to be 10^{17}–10^{19} cm^{-3} in the whiskers and related to *p*-type dopants in the SiC. For all types of electrodes, the electrode semicircle was unstable at room temperature and grew with time. Reducing the whisker content in the composite increased the resistance and decreased the capacitance associated with the electrodes by factors that were agreeable with the percolation-network sensitivity proposed above. Also, the dc-bias dependencies of both the resistance and relaxation time associated with the electrode

semicircle were exponential and were related through the equivalent circuit model. However, for sputtered electrodes these exponential dependences are often so weak that they appear linear. This is because sputtered contacts contribute little to the total resistance and thus (by Kirchoff's Voltage Law) only a small fraction of the applied bias is applicable to the electrode response. Correction factors were needed to obtain reasonable estimates of the Schottky barrier height as 0.2–1.6 eV for sputtered Ag. Figure 14c shows a proposed band diagram for Schottky barriers at the opposing electrical contacts, assuming p-type conductivity dominates the bulk whisker network.

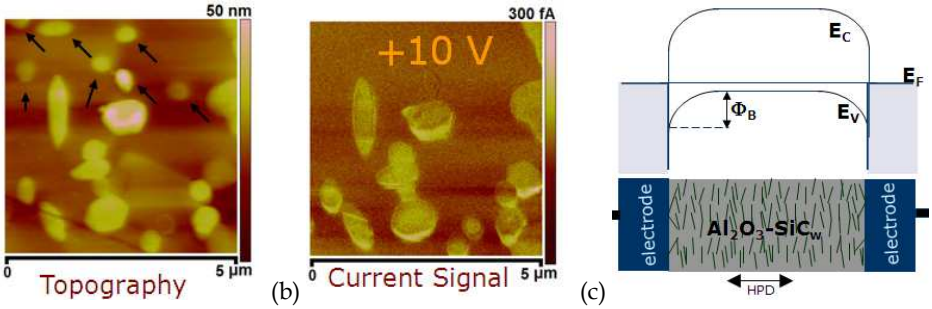

(a) (b) (c)

Fig. 14. (a) Topography of 20 vol% SiC_w composite surface scanned by an atomic force microscope. (b) Current signal from a scan on the same area using a 10 V dc bias, showing the absence of the SiC_w marked with arrows in 'a'. (c) Simple equilibrium band diagram model for symmetrical Schottky barriers at the electrodes of bulk samples. *Source for (a-b):* Bertram & Gerhardt, 2009. Copyright American Institute of Physics.

3.8. Effects of Whisker Defect Structures and Interfaces on Various Properties

In Al_2O_3-SiC_w composites, the whiskers are the most important phase because they have the greatest influence on the composite properties. These properties can therefore be expected to significantly depend on defects within the SiC whiskers and whisker interfaces with the matrix and each other. However, when incorporated in composites, it may be difficult to separate these effects from those related to characteristics of the microstructure previously described in Section 3.5. Nevertheless, such issues are worthy of discussion.

To this end, one must first know that the hot-pressing process and the sintering process which follows extrusion are conducted at high temperatures (~1600-1800°C). There is reason to believe that the chemical compositions of the SiC_w are altered during such high temperature processes and this is of interest because it might affect intra- and inter-whisker transport and microwave dielectric loss. Energy dispersive x-ray spectroscopy of whisker surfaces in composites hot-pressed at 1600°C suggest aluminum diffusion from Al_2O_3 into the whiskers to a concentration of 1-2 atomic percent (Zhang et al., 1996). This suggests very high p-type (semiconductive) doping and is expected to affect both electrical and thermal conductivity. Since this doping level persisted throughout the full measurement depth of ~350 nm into the whisker, a value on the order of the typical whisker diameter, one might infer that this doping is achieved throughout entire whisker cross sections. Evidence of aluminum doping has also been found in similar composites of liquid-phase sintered silicon carbide which used alumina as a sintering aid. However, in these studies the Al doping was

only found around the rims of the SiC grains and did not persist into the grain cores (Sanchez-Gonzalez et al., 2007).

In another study, it was found that high-frequency dielectric loss of certain SiC composites decreases with increasing concentrations of aluminum and nitrogen dopants in the SiC (Zhang et al., 2002). These results can be understood in terms of the proposed underlying mechanism of dielectric loss in SiC: dipole relaxation and/or reorientation of vacancy (V_C-V_{Si}) and antisite (Si_C-C_{Si}) defect pairs. Smaller concentrations of such defects are expected as temperature decreases or impurity concentration increases in the SiC_w.

Another possible electrical issue is scattering of charge carriers at stacking faults within the SiC_w. One might expect that the short-spacing between faults would severely limit the mean free path of carriers and therefore the mobility and conductivity of the SiC_w. Also, band-structure calculations reveal that stacking faults in SiC introduce states inside the bandgap which are localized at about 0.2 eV below the conduction band (Iwata et al., 2002). Due to this position relative to the band edges, it was concluded that stacking faults hinder electron transport in n-type SiC but not hole transport in p-type SiC. As they noted, this assertion is the only way to rationalize other experimental results which show that SiC electrical resistivity strongly depends on transport direction relative to stacking-fault orientation for n-type SiC but not for p-type SiC (Takahashi et al., 1997). This result may be applicable to Al_2O_3-SiC_w composites since the SiC_w might be doped during high-temperature composite fabrication. Since SiC is a wide-bandgap semiconductor, one would naturally expect the doping of the SiC whiskers to determine their electrical conductivity and influence the electrical response of composites which contain them.

In a study of the internal potential fluctuations associated with the stacking faults in SiC nanowires, the wires were considered as alternating stacks of perfect crystal and defective regions based on stacking-fault observation during TEM investigation (Yoshida et al., 2007). The position-dependence of the inner potential of the SiC rods was measured by electron holography and correlated to the perfect-crystal and defective regions. The perfect crystal regions had significantly lower inner potential. They speculated that Al-P impurity segregation occurred and led to the self-organized formation of p-n junctions along the lengths of the SiC nanowires. If true, this would certainly affect the electrical response of the SiC wires themselves and likely also that of ensembles of such wires in composites.

Additionally, at high temperatures, β-SiC is known to undergo a phase transformation to form the α-SiC and this is relevant to ceramic-processing aspects of making the composites because the two polytypes tend to exhibit different morphologies. One study investigated this process in the 1925-2000°C range (Nader et al., 1999). The transformation rate decreased as the reaction proceeded such that the kinetics are adequately described by a nucleation-and-growth equation for α-SiC grain growth based on the general equation developed by Johnson and Mehl for grain growth processes. Also, the reaction was found to be "slow" (only 94% completion after 14 hours) and was affected by the chemical composition (impurities and non-stoichiometry) of the SiC crystallite.

It has also been found that coating SiC_w prior to inclusion in composites can provide improved properties and cutting-tool performance. Such high-performance tools may be

obtained from Greenleaf Corporation. In one study, precoating the SiC_w with alumina by an aqueous precipitation technique allowed for better dispersion during ultrasonic mixing in ethanol (Kato et al., 1995). The more-homogeneous mixing resulted in improved sintered density and improved mechanical strength. In another study, carbon coatings were applied to SiC_w and the resulting composites exhibited improved fracture resistance, possibly due to reduced residual thermal stresses from post-sintering cool down (Thompson & Krstic, 1993).

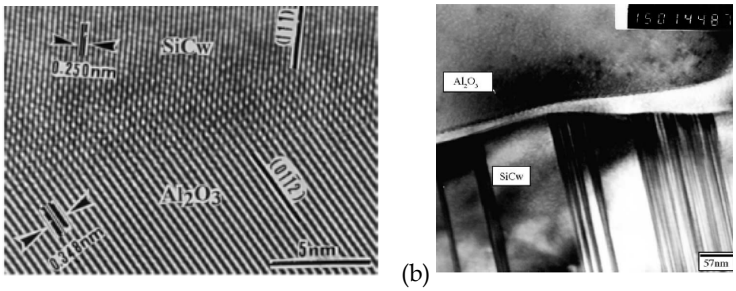

(a) (b)

Fig 15. (a) High-resolution TEM image of clean whisker-matrix interface in a composite made from whiskers etched in HF prior to hot-pressing. (b) TEM image showing a glassy coating formed after hot-pressing due to residual oxygen on the whisker surface. *Sources:* (a) F. Ye et al., 2000. (b) V. Garnier et al., 2005. Copyright Elsevier.

The whisker-matrix interface seems to determine to what extent the thermal-expansion difference between Al_2O_3 and SiC_w dictates the stress distributions in the composites. Because the alumina matrix has a higher thermal expansion coefficient compared to the SiC whiskers, the matrix is in tension and the SiC_w are in compression upon cooling from hot-pressing temperatures (Becher et al., 1995). However, it has also been proposed that matrix→SiC_w stress transfer can explain observations of (tensile) whisker fracture instead of pullout: specifically, that the higher-modulus SiC whiskers unload the matrix and reduce stress around defects in the composite microstructure and result in an overall improvement in composite mechanical properties (Björk & Hermansson, 1989). The mechanical stress distribution within the SiC whiskers might also affect electrical response of composites because elastic strain was found to result in changes in electrical response of β-SiC films and used to explain the observed back-to-back Schottky-barrier response (Rahimi et al., 2009).

It thus seems that the interfaces of whiskers with neighboring materials are of considerable importance. Even without coatings, it has been found that treating whisker surfaces to control surface chemistry prior to composite fabrication can increase final-composite toughness from 4.0 up to 9.0 $MPa \cdot m^{1/2}$. This study used different gas mixtures during heat treatments of whiskers and it was found that reducing the residual oxygen and silica on whisker surfaces resulted in the highest fracture toughness (Homeny et al., 1990). Free carbon and silicon nitride on surfaces resulted in lower toughness, and silicon dioxide resulted in the lowest. In another work, pretreating whiskers with an HF acid etch caused surface smoothening and a reduction in residual oxygen and other impurities on whisker surfaces (Ye et al., 2000). This led to a relatively clean SiC-alumina interface in the fabricated composites, as shown in Figure 15a. Without such cleaning, it is common for amorphous

interfacial phases composed of Al, Si, and O to form around the whiskers during hot pressing and this generally results in composites exhibiting inhibited whisker pull-out, crack bridging, and deflection due to excessively-high interfacial bonding strength. An example of such a glassy phase coating a whisker is shown in Figure 15b and was correlated to a fracture toughness reduced by 22% (Garnier et al., 2005).

4. Conclusions and Future Work

A great deal of research has been conducted on Al_2O_3-SiC_w composites to understand the basic physical processes on which their successful applications in cutting-tool inserts and microwave cooking are based. The initial reason for development of these materials, an application in ceramic engines, did not appear to pan out due to insufficient stability under conditions of high-temperature and stress. Future investigators might attempt to improve properties of the composites by applying principles covered in this chapter (and elsewhere) to more carefully control the microstructure of the composites. It has already been seen that use of whisker coatings can significantly improve mechanical performance. As the electrical application has motivated the most recent work, it may be interesting to investigate the effects of sintering additives and controlled whisker doping on electrical response. Alternatively, one might be able to manipulate the SiC_w aspect-ratio distribution to reduce the percolation threshold. Finally, improvements in microwave sintering of larger ceramic-composite parts having tuned dielectric properties might lead to interesting applications.

Acknowledgements

This work was funded by the National Science Foundation under DMR-0604211. BDB received some additional support from a Presidential Fellowship from Georgia Tech and a Shackelford Fellowship from Georgia Tech Research Institute. Advanced Composite Materials LLC and Greenleaf Corporation are thanked for images and sharing expertise about the applications.

5. References

ACM website. http://www.acm-usa.com/whiskers-properties.html. 10/13/2010.

Amateau, M.; Stutzman, B; Conway, J. & Halloran, J. "Performance of laminated ceramic composite cutting tools." *Ceramics International,* Vol. 21, No. 5, (1995) 317-323.

Balberg, I.; Anderson, C.; Alexander, S. & Wagner, N. "Excluded volume and its relation to the onset of percolation." *Physical Review B,* Vol. 30, No. 7, (1984) 3933-3943.

Balberg, I.; D. Azulay, D.; Toker, D. & Millo, O. "Percolation and tunneling in composite materials," *International Journal of Modern Physics B,* Vol. 18, No. 15, (2004) 2091-2121.

Basak, T. & Priya, A. "Role of ceramic supports on microwave heating of materials." *Journal of Applied Physics,* Vol. 97, No. 8, (2005) 083537.

Becher, P.; Angelini, P.; Warwick, W. & Tiegs, T. "Elevated-temperature delayed failure of alumina reinforced with 20 vol% silicon-carbide whiskers." *Journal of the American Ceramic Society,* Vol. 73, No. 1, (1990) 91-96.

Becher, P.; Hsueh, C.; Angelini, P. & Tiegs, T. "Theoretical and experimental analysis of the toughening behavior of whisker reinforcement in ceramic matrix composites." *Materials Science and Engineering A-Structural Materials Properties Microstructure and Processing,* Vol. 107, (1989) 257-259.

Becher, P.; Hsueh, C.; Angelini, P. & Tiegs, T. "Toughening behavior in whisker-reinforced ceramic matrix composites." *Journal of the American Ceramic Society*, Vol. 71, No. 12, 1050-61 (1988).

Becher, P.; Hsueh, C.; & Waters, S. "Thermal-expansion anisotropy in hot-pressed SiC-whisker-reinforced alumina composites." *Materials Science and Engineering a-Structural Materials Properties Microstructure and Processing,* Vol. 196, No. 1-2, (1995) 249-251.

Becher, P. & Wei, G. "Toughening behavior in SiC-whisker-reinforced alumina." *Journal of the American Ceramic Society,* Vol. 67, No. 12, (1984) C267-C269.

Bertram, B. & Gerhardt, R. "Room temperature properties of electrical contacts to alumina composites containing silicon carbide whiskers." *Journal of Applied Physics,* Vol. 105, No. 7, (2009) 074902.

Bertram, B. & Gerhardt, R. "Effects of frequency, percolation, and axisymmetric microstructure on the electrical response of hot-pressed alumina-silicon carbide whisker composites." *J. Am. Ceram. Soc.,* (2010) accepted.

Billman, E.; Mehrotra, P.; Shuster, A. & Beeghly, C. "Machining with Al_2O_3-SiC-whisker cutting tools." *American Ceramic Society Bulletin,* Vol. 67, No. 6, (1988) 1016-1019.

Björk, L. & Hermansson, L. "Hot Isostatically Pressed Alumina-Silicon Carbide-Whisker Composites." *Journal of the American Ceramic Society,* Vol. 72, No. 8, (1989) 1436-1438.

Budiansky, B. & O'Connell, R. "Elastic moduli of a cracked solid." *International Journal of Solids and Structures,* Vol. 12, No. 2, (1976) 81-97.

Calame, J.; Abe, D.; Levush, B. & Danly, B.; "Variable temperature measurements of the complex dielectric permittivity of lossy AlN-SiC composites from 26.5-40 GHz." *Journal of Applied Physics,* Vol. 89, No. 10, (2001) 5618-5621.

Carter, J. "Proposed Energy Policy for United States." (televised speech) 1977.

Cole, K. & Cole, R. "Dispersion and absorption in dielectrics I. Alternating current characteristics." *Journal of Chemical Physics,* Vol. 9, No. 4, (1941) 341-351.

Collin, M. & Rowcliffe, D. "Influence of thermal conductivity and fracture toughness on the thermal shock resistance of alumina-silicon-carbide-whisker composites." *Journal of the American Ceramic Society,* Vol. 84, No. 6, (2001) 1334-1340.

Connor, M.; Roy, S.; Ezquerra, T. & Baltá Calleja, F. "Broadband ac conductivity of conductor-polymer composites," *Physical Review B,* Vol. 57, No. 4, (1998) 2286.

de Arellano-Lopez, A.; Cumbrera, F.; Dominguez-Rodriguez, A.; Goretta, K. & Routbort, J. "Compressive creep of SiC-whisker-reinforced Al_2O_3." *Journal of the American Ceramic Society,* Vol. 73, No. 5, (1990) 1297-1300.

de Arellano-López, A.; Domínguez-Rodríguez, A.; Goretta, K. & Routbort, J. "Plastic deformation mechanisms in SiC-whisker-reinforced alumina." *Journal of the American Ceramic Society,* Vol. 76, No. 6, (1993) 1425-1432.

de Arellano-Lopez, A.; Dominguez-Rodriguez, A. & Routbort, J. "Microstructural constraints for creep in SiC-whisker-reinforced Al_2O_3." *Acta Materialia,* Vol. 46, No. 18, (1998) 6361-6373.

de Arellano-Lopez, A.; Melendez-Martinez, J.; Dominguez-Rodriguez, A. & Routbort, J. "Creep of Al_2O_3 containing a small volume fraction of SiC-whiskers." *Scripta Materialia,* Vol. 42, No. 10, (2000) 987-991.

de Arellano-Lopez, A.; Melendez-Martinez, J.; Dominguez-Rodriguez, A.; Routbort, J.; Lin, H. & Becher, P. "Grain-size effect on compressive creep of silicon-carbide-whisker-reinforced aluminum oxide." *Journal of the American Ceramic Society,* Vol. 84, No. 7, (2001) 1645-1647.

DeHoff, R. (1993). *Thermodynamics in materials science*, McGraw-Hill, ISBN 0070163138,New York.

Dogan, C. & Hawk, J. "Influence of whisker toughening and microstructure on the wear behavior of Si_3N_4- and Al_2O_3-matrix composites reinforced with SiC." *Journal of Materials Science,* Vol. 35, No. 23, (2000) 5793-5807.

Fabbri, L.; Scafe, E. & Dinelli, G. "Thermal and elastic properties of alumina-silicon carbide whisker composites." *Journal of the European Ceramic Society,* Vol. 14, No. 5, (1994) 441-446.

Farkash, M. & Brandon, D. "Whisker alignment by slip extrusion." *Materials Science and Engineering A-Structural Materials Properties Microstructure and Processing,* Vol. 177, No. 1-2, (1994) 269-275.

Ford, G. "Address on the State of the Union before a Joint Session of the 94th Congress." (1975).

Garnier, V.; Fantozzi, G.; Nguyen, D.; Dubois, J. & Thollet, G. "Influence of SiC whisker morphology and nature of SiC/Al_2O_3 interface on thermomechanical properties of SiC reinforced Al_2O_3 composites." *Journal of the European Ceramic Society,* Vol. 25, No. 15, (2005) 3485-3493.

Gerhardt, R. "Impedance Spectroscopy and Mobility Spectra," *Encyclopedia of Condensed Matter Physics*. Elsevier, (2005) 350-363.

Gerhardt, R. & Ruh, R. "Volume fraction and whisker orientation dependence of the electrical properties of SiC-whisker-reinforced mullite composites." *Journal of the American Ceramic Society,* Vol. 84, No. 10, (2001) 2328-2334.

Gerhardt, R.; Runyan, J.; Sana, C.; McLachlan, D. & Ruh, R. "Electrical Properties of Boron Nitride Matrix Composites: III, Observations near the Percolation Threshold in BN-B_4C Composites" *Journal of the American Ceramic Society*, Vol. 84, No. 10, (2001) 2335-42.

Goncharenko, A. "Generalizations of the Bruggeman equation and a concept of shape-distributed particle composites." *Physical Review E,* Vol. 68, No. 4. (2003) 041108.

Holm, E. & Cima, M. " Two-Dimensional Whisker Percolation in Ceramic-Matrix Ceramic-Whisker Composites." *Journal of the American Ceramic Society,* Vol. 72, No. 2, (1989) 303-305.

Homeny, J. & Vaughn, W. & Ferber, M. "Silicon-carbide whisker alumina matrix composites – Effect of whisker surface treatment on fracture toughness." *Journal of the American Ceramic Society,* Vol. 73, No. 2, (1990) 394-402.

Iio, S.; Watanabe, M.; Matsubara, M. & Matsuo, Y. "Mechanical properties of alumina silicon-carbide whisker composites." *Journal of the American Ceramic Society,* Vol. 72, No. 10, (1989) 1880-1884.

Iwata, H.; Lindefelt, U.; Oberg, S. & Briddon, P. "Localized electronic states around stacking faults in silicon carbide." *Physical Review B,* Vol. 65, No. 3, (2002) 033203.

Jakus, K. & Nair, S. "Nucleation and growth of cracks in SiC/Al_2O_3 composites." *Composites Science and Technology,* Vol. 37, No. 1-3, (1990) 279-297.

Jones, R. (1999) *Mechanics of Composite Materials*, Taylor & Francis, ISBN 156032712X, Philadelphia, PA.

Jonscher, A. (1983). *Dielectric Relaxation in Solids*, Chelsea Dielectrics Press Ltd., ISBN 0950871109, London.

Karunanithy, S. "Chemical processes that degrade composites of alumina with SiC whiskers." *Materials Science and Engineering A-Structural Materials Properties Microstructure and Processing,* Vol. 112, (1989) 225-231.

Kato, A.; Nakamura, H.; Tamari, N.; Tanaka, T. & Kondo, I. "Usefulness of alumina-coated SiC whiskers in the preparation of whisker-reinforced alumina ceramics." *Ceramics International,* Vol. 21, No. 1, (1995) 1-4.

Kim, H. & Moorhead, A. "Oxidation behavior and effects of oxidation on the strength of SiC-whisker reinforced alumina."*Journal of Materials Science,* Vol. 29, No. 6, (1994) 1656-1661.

Lagarkov, A.; Matytsin, S.; Rozanov, K. & Sarychev, A. "Dielectric permittivity of fiber-filled composites: comparison of theory and experiment." *Physica A,* Vol. 241, No. 1-2, (1997) 58-63.

Lagarkov, A.; Matytsin, S.; Rozanov, K. & Sarychev, A. "Dielectric properties of fiber-filled composites." *Journal of Applied Physics,* Vol. 84, No. 7, (1998) 3806-3814.

Lagarkov, A. & Sarychev, A. "Electromagnetic properties of composites containing elongated conducting inclusions." *Physical Review B,* Vol. 53, No. 10, (1996) 6318-6336.

Lee, K. & Sheargold, S. "Particulate matters in silicon-carbide whiskers." *American Ceramic Society Bulletin,* Vol. 65, No. 11, (1986) 1477-1477.

Lee, W. & Case, E. "Cyclic thermal shock in SiC-whisker-reinforced alumina composite." *Materials Science and Engineering A-Structural Materials Properties Microstructure and Processing,* Vol. 119 (1989) 113-126.

Li, X. "Ceramic Cutting Tools - An Introduction." *Key Engineering Materials,*Vol. 96, (1994) 1-18.

Lin, H.; Alexander, K. & Becher, P. "Grain size effect on creep deformation of alumina-silicon carbide composites." *Journal of the American Ceramic Society,* Vol. 79, No. 6, (1996) 1530-1536.

Lin, H. & Becher, P. "Creep behavior of a SiC-whisker-reinforced alumina." *Journal of the American Ceramic Society,* Vol. 73, No. 5, (1990) 1378-1381.

Lin, H. & Becher, P. "High-temperature creep deformation of alumina SiC-whisker composites." *Journal of the American Ceramic Society,* Vol. 74, No. 8, (1991) 1886-1893.

Lipetzky, P.; Nutt, S.; Koester, D. & Davis, R. "Atmospheric effects on compressive creep of SiC-whisker-reinforced alumina." *Journal of the American Ceramic Society,* Vol. 74, No. 6, (1991) 1240-1247.

Luthra, K. & Park, H. "Oxidation of silicon carbide-reinforced oxide-matrix composites at 1375°C to 1575°C." *Journal of the American Ceramic Society,* Vol. 73, No. 4, (1990) 1014-1023.

Mallick, P. (2008). *Fiber-Reinforced Composites*, CRC Press, ISBN 0849342058, Dearborn, MI.

McCluskey, P.; Williams, R.; Graves, R. & Tiegs, T. "Thermal diffusivity/conductivity of alumina-silicon carbide composites." *Journal of the American Ceramic Society,* Vol. 73, No. 2, (1990) 461-464.

McLachlan, D. "Analytic scaling functions for percolative metal-insulator phase transitions fitted to Al_xGe_{1-x} data." *Physica B,* Vol. 254, No. 3-4, (1998) 249-255.

Mebane, D. & Gerhardt, R. "Orientation Dependence of Resistivity in Anisotropic Ceramic Composites." *Ceramic Transactions,* Vol. 150, (2004) 265-272.

Mebane, D. & Gerhardt, R. "Interpreting impedance response of silicon carbide whisker/alumina composites through microstructural simulation." *Journal of the American Ceramic Society,* Vol. 89, No. 2, (2006) 538-543.

Mebane, D.; Gokhale, A. & Gerhardt, R., "Trivariate, stereological length-radius-orientation unfolding derived and applied to alumina-silicon carbide whisker composites." *Journal of the American Ceramic Society,* Vol. 89, No. 2, (2006) 620-626.

Mehrotra, P. "Applications of ceramic cutting tools." *Advanced Ceramic Tools for Machining Application - Iii,"* Vol. 138, No. 1, (1998) 1-24.

Metaxas, A. & Meredith, R. (1983). *Industrial Microwave Heating*. Peter Peregrinus Ltd. on behalf of the Institution of Electrical Engineers, ISBN 0906048893, London.

Mukae, K.; Tsuda, K. & Nagasawa, I. "Capacitance-vs-voltage characteristics of ZnO varistors." *Journal of Applied Physics,* Vol. 50, No. 6, (1979) 4475-4476.

Nader, M.; Aldinger, F. & Hoffmann, M. "Influence of the alpha/beta-SiC phase transformation on microstructural development and mechanical properties of liquid phase sintered silicon carbide." *Journal of Materials Science,* Vol. 34, No. 6, (1999) 1197-1204.

Nutt, S. "Defects in silicon carbide whiskers," *Journal of the American Ceramic Society,* Vol.67, No. 6, (1984) 428-431.

Nutt, S. " Microstructure and growth model for rice-hull-derived SiC whiskers." *Journal of the American Ceramic Society,* Vol. 71, No. 3, (1988) 149-156.

Nutt, S.; Lipetzky, P. & Becher, P. "Creep deformation of alumina-SiC composites." *Materials Science and Engineering A-Structural Materials Properties Microstructure and Processing,* Vol. 126, (1990) 165-172.

Nutt, S. & Lipetzky, P. "Creep deformation of whisker-reinforced alumina." Materials Science and Engineering A, Vol. 166, (1993) 199-209.

O'Meara, C.; Suihkonen, T.; Hansson, T. & Warren, R. "A microstructural investigation of the mechanisms of tensile creep deformation in an Al_2O_3/SiC_w composite." *Materials Science and Engineering a-Structural Materials Properties Microstructure and Processing,* Vol. 209, No. 1-2, (1996) 251-259.

Panteny, S.; Stevens, R. & Bowen, C. "The frequency dependent permittivity and ac conductivity of random electrical networks." *Ferroelectrics,* Vol. 319, (2005) 199-208.

Park, H.; Kim, H. & Kim, D. "Evaluation of whisker alignment in axisymmetrical SiC_w-reinforced Al_2O_3 composite materials." *Journal of the American Ceramic Society,* Vol. 77, No. 11, (1994) 2828-2832.

Parris, P. & Kenkre, V."Thermal runaway in ceramics arising from the temperature dependence of the thermal conductivity." *Physica Status Solidi B-Basic Research,* Vol. 200, No. 1, (1997) 39-47.

Peng, X.; Zhang, Y.; Huang, X.; Song, L. & Hu, X. "Nitrogen corrosion in silicon carbide whisker-reinforced alumina composites." *Advanced Engineering Materials,* Vol. 2, No. 7, (2000) 448-450.

Porter, L. & Davis, R. "A critical review of ohmic and rectifying contacts for silicon carbide." *Mater. Sci. Eng. B,* Vol. 34, No. 2-3, (1995) 83-105.

Quan, G.; Conlon, K. & Wilkinson, D. "Investigation of anelastic creep recovery in SiC whisker-reinforced alumina composites." *Journal of the American Ceramic Society,* Vol. 88, No. 11, (2005) 3104-3109.

Quantrille, T. (2007) "Novel Composite Structures for Microwave Heating and Cooking." Proceedings of 41st Annual Microwave Symposium. Vancouver, BC, 2007, International Microwave Power Institute.

Quantrille, T. (2008) "Ceramic Composites for Microwave Grilling and Speed Cooking." Proceedings of 42nd Annual Microwave Symposium, New Orleans, LA, 2008, International Microwave Power Institute.

Rahimi, R.; Miller, C.; Raghavan, S.; Stinespring, C. & Korakakis, D. "Electrical properties of strained nano-thin 3C-SiC/Si heterostructures." *Journal of Physics D-Applied Physics,* Vol. 42, No. 5, (2009) 055108.

Raj, R. & Ashby, M. "Grain boundary sliding and diffusional creep." *Metallurgical Transactions,* Vol. 2, No. 4, (1971) 1113.

Raju, C. & Verma, S. "SiC whiskers from rice hulls: formation, purification, and characterisation." *British Ceramic Transactions,* Vol. 96, No. 3, (1997) 112-115.

Rice, R. (2003). *Ceramic Fabrication Technology*, Marcel Dekker, ISBN 0824708539, New York, NY.

Richerson, D. (1992) *Modern Ceramic Engineering*, Marcel Dekker, ISBN 1574446932, New York, NY.

Rodelsperger, K. & Bruckel, B. "The Carcinogenicity of WHO fibers of silicon carbide: SiC whiskers compared to cleavage fragments of granular SiC." *Inhalation Toxicology,* Vol. 18, No. 9, (2006) 623-631.

Ruh, R. & Chizever, H. "Permittivity and permeability of mullite-SiC-whisker and spinel-SiC-whisker composites." *Journal of the American Ceramic Society,* Vol. 81, No. 4, (1998) 1069-1070.

Runyan, J.; Gerhardt, R. & Ruh, R. "Electrical properties of boron nitride matrix composites: I, analysis of McLachlan equation and modeling of the conductivity of boron nitride-boron carbide and boron nitride-silicon carbide composites." *Journal of the American Ceramic Society,* Vol. 84, No. 7, (2001a) 1490-1496.

Runyan, J.; Gerhardt, R. & & Ruh, R. "Electrical properties of boron nitride matrix composites: II, dielectric relaxations in boron nitride-silicon carbide composites." *Journal of the American Ceramic Society,* Vol. 84, No. 7, (2001b) 1497-1503.

Russell, L.M.; Johnson, L.F.; Hasselman, D.P.H. & Ruh, R. "Thermal Conductivity/Diffusivity of Silicon Carbide Whisker Reinforced Mullite." *Journal of the American Ceramic Society*, Vol. 70, No. 10, (1987) C226-C229.

Salganik, R. "Mechanics of bodies with many cracks." *Mechanics of Solids,* Vol. 8, No. 4, (1973) 135-143.

Sanchez-Gonzalez, J.; Ortiz, A.; Guiberteau, F. & Pascual, C. "Complex impedance spectroscopy study of a liquid-phase-sintered alpha-SiC ceramic." *Journal of the European Ceramic Society,* Vol. 27 (2007) 3935-3939.

Sandlin, M.; Lee, E. & Bowman, K. "Simple geometric model for assessing whisker orientation in axisymmetrical SiC-whisker-reinforced composites." *Journal of the American Ceramic Society,* Vol. 75, No. 6, (1992) 1522-1528.

Sheng, P.; Sichel, E. & Gittleman, J. "Fluctuation-induced tunneling conduction in carbon-polyvinychloride composites." *Physical Review Letters,* Vol. 40, No. 18, (1978) 1197-1200.

Shimoo, T.; Okamura, K. & Morisada, Y. "Active-to-passive oxidation transition for polycarbosilane-derived silicon carbide fibers heated in Ar-O_2 gas mixtures." *Journal of Materials Science,* Vol. 37, No. 9, (2002) 1793-1800.

Sillars, R. "The Properties of a Dielectric Containing Semiconducting Particles of Various Shapes." *J. Inst. Elect. Engrs.,* Vol. 80, (1937) 378-394.

Singh, P.; Selvam, A. & Nair, N. "Synthesis of SiC whiskers from a mixture of rice husks and coconut shells." *Advances in Powder Metallurgy & Particulate Materials,* Vol. 3-53 (1998) 53-64.

Sinott, M. (1987) "Ceramic Technology for Advanced Heat Engines." Edited by N. R. C. National Materials Advisory Board. Washington D.C.

Stauffer, D. & Aharony, A. (1994). Introduction to Percolation Theory: Revised Second Edition, CRC Press, ISBN 0748402535, London and Philadelphia.

Streetman, B. & Banerjee, S. (2000) *Solid State Electronic Devices*, Prentice Hall, Inc. ISBN 013149726X, Upper Saddle River, NJ.

Tai, Q. & Mocellin, A. "Review: High temperature deformation of Al_2O_3-based ceramic particle or whisker composites." *Ceramics International,* Vol. 25, No. 5, (1999) 395-408.

Takahashi, J.; Ohtani, N.; Katsuno, M. & Shinoyama, S. "Sublimation growth of 6H- and 4H-SiC single crystals in the [1 $\bar{1}$ 00] and [11 $\bar{2}$ 0] directions," *Journal of Crystal Growth,* Vol. 181, No. 3, (1997) 229-240.

Takahashi, K.; Yokouchi, M.; Lee, S. & Ando, K. "Crack-healing behavior of Al_2O_3 toughened by SiC whiskers." *Journal of the American Ceramic Society,* Vol. 86, No. 12, (2003) 2143-2147.

Taya, M. (2005). Electronic Composites: Modeling, Characterization, Processing, and Applications, Cambridge University Press, ISBN 0521057318, Cambridge.

Thangaraj, A. & Weinmann, K. "On the wear mechanisms and cutting performance of silicon-carbide whisker-reinforced alumina." *Journal of Engineering for Industry-Transactions of the ASME,* Vol. 114, No. 3, (1992) 301-308.

Thompson, I. & Krstic, V. "Effect of carbon coating on mechanical strength of SiC whisker-reinforced alumina composites." *Theoretical and Applied Fracture Mechanics,* Vol. 19, No, 1, (1993) 61-67.

Tian, W. & Yang, R. "Effect of interface scattering on phonon thermal conductivity percolation in random nanowire composites." *Applied Physics Letters,* Vol. 90, No. 26, (2007) 263105.

Tiegs, T. & Becher, P. "Thermal shock behavior of an alumina-SiC whisker composite." *Journal of the American Ceramic Society,* Vol. 70, No. 5, (1987) C109-C111.

Tsangaris, G.; Kouloumbi, N. & Kyvelidis, S. "Interfacial relaxation phenomena in particulate composites of epoxy resin with copper or iron particles." *Materials Chemistry and Physics,* Vol. 44, No. 3, (1996) 245-250.

Vaughan, G. & Trently, S. "The toxicity of silicon carbide whiskers: a review." *Journal of Environmental Science and Health Part a-Environmental Science and Engineering & Toxic and Hazardous Substance Control,* Vol. 31, No. 8, (1996) 2033-2054.

von Hippel, A. (1954). *Dielectrics and Waves*, Wiley, ISBN 1580531229, New York, NY.

Wagner, R. & Ellis, W. "Vapor-liquid-solid mechanism of single crystal growth." *Applied Physics Letters,* Vol. 4, No. 5, (1964) 89-90.

Wang, C.; Huang, Y.; Li, Y.; Zhang, Z.; Xie, Z. & Li, J. "Resistivity controlled by SiC whisker orientation in Si_3N_4 matrix composites." *Journal of Materials Science Letters,* Vol. 17, No. 10, (1998) 829-831.

Wang, D. & Lopez, H. "Morphological and kinetic aspects of thermal-oxidation of SiC whisker-reinforced Al_2O_3." *Materials Science and Technology,* Vol. 10, No. 10, (1994) 879-885.

Wang, P.; Hsu, S. & Wittberg, T. "Oxidation kinetics of silicon carbide whiskers studied by x-ray photoelectron spectroscopy." *Journal of Materials Science,* Vol. 26, No. 6, (1991) 1655-1658.

Wu, J. & McLachlan, D. "Scaling behavior of the complex conductivity of graphite-boron nitride percolation systems." *Physical Review B,* Vol. 58, No. 22, (1998) 14880.

Ye, F.; Lei, T. & Zhou, Y. "Interface structure and mechanical properties of Al_2O_3-20vol%SiC_w ceramic matrix composite." *Materials Science and Engineering A-Structural Materials Properties Microstructure and Processing,* Vol. 281, No. 1-2, (2000) 305-309.

Yoshida, H.; Kohno, H.; Ichikawa, S.; Akita,T. & Takeda, S. "Inner potential fluctuation in SiC nanowires with modulated interior structure." *Materials Letters,* Vol. 61, No. 14-15, (2007) 3134-3137.

Zhang, B.; Li, J.; Sun, J.; Zhang, S.; Zhai, H. & Du, Z. "Nanometer silicon carbide powder synthesis and its dielectric behavior in the GHz range." *Journal of the European Ceramic Society,* Vol. 22, No. 1, (2002) 93-99.

Zhang, J.; Huang, H.; Cao, L.; Xia, F. & Li, G. "Semiconductive property and impedance spectra of alumina silicon-carbide whisker composite." *Journal of the American Ceramic Society,* Vol. 75, No. 8, (1992) 2286-2288.

Zhang, Z.; Shan, H.; Huang, Y. & Jiang, Z. "Characterisation of interfacial bonding in Al_2O_3 coated SiC whisker reinforced TZP composites." *British Ceramic Transactions,* Vol. 95, No. 3, (1996) 125-128.

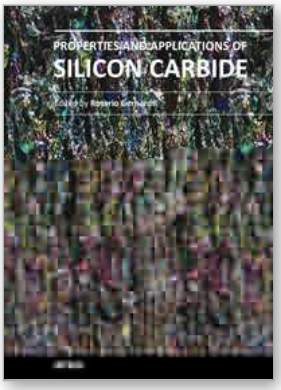

Properties and Applications of Silicon Carbide

Edited by Prof. Rosario Gerhardt

ISBN 978-953-307-201-2
Hard cover, 536 pages
Publisher InTech
Published online 04, April, 2011
Published in print edition April, 2011

In this book, we explore an eclectic mix of articles that highlight some new potential applications of SiC and different ways to achieve specific properties. Some articles describe well-established processing methods, while others highlight phase equilibria or machining methods. A resurgence of interest in the structural arena is evident, while new ways to utilize the interesting electromagnetic properties of SiC continue to increase.

How to reference

In order to correctly reference this scholarly work, feel free to copy and paste the following:

Brian Bertram and Rosario Gerhardt (2011). Properties and Applications of Ceramic Composites Containing Silicon Carbide Whiskers, Properties and Applications of Silicon Carbide, Prof. Rosario Gerhardt (Ed.), ISBN: 978-953-307-201-2, InTech, Available from: http://www.intechopen.com/books/properties-and-applications-of-silicon-carbide/properties-and-applications-of-ceramic-composites-containing-silicon-carbide-whiskers

INTECH
open science | open minds

InTech Europe
University Campus STeP Ri
Slavka Krautzeka 83/A
51000 Rijeka, Croatia
Phone: +385 (51) 770 447
Fax: +385 (51) 686 166
www.intechopen.com

InTech China
Unit 405, Office Block, Hotel Equatorial Shanghai
No.65, Yan An Road (West), Shanghai, 200040, China
中国上海市延安西路65号上海国际贵都大饭店办公楼405单元
Phone: +86-21-62489820
Fax: +86-21-62489821